

NAVAL POSTGRADUATE SCHOOL
Monterey, California



THEESIS

ORBITAL PERTURBATION ANALYSIS OF EARTH-CROSSING ASTEROIDS

by

Wade E. Knudson

December 1995

Thesis Advisor:

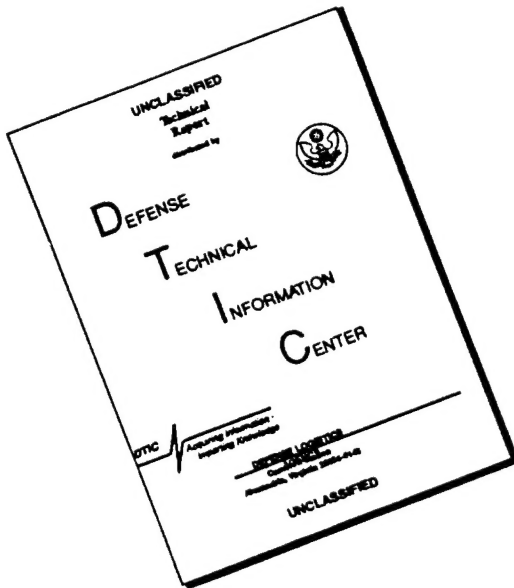
L. Michael Ross

Approved for public release; distribution is unlimited.

19960412 127

DATA ON A NEWLY ESTABLISHED INDUSTRIAL STATE

DISCLAIMER NOTICE



THIS DOCUMENT IS BEST
QUALITY AVAILABLE. THE COPY
FURNISHED TO DTIC CONTAINED
A SIGNIFICANT NUMBER OF
PAGES WHICH DO NOT
REPRODUCE LEGIBLY.

REPORT DOCUMENTATION PAGE

Form Approved OMB No. 0704-0188

Public reporting burden for this collection of information is estimated to average 1 hour per response, including the time for reviewing instruction, searching existing data sources, gathering and maintaining the data needed, and completing and reviewing the collection of information. Send comments regarding this burden estimate or any other aspect of this collection of information, including suggestions for reducing this burden, to Washington Headquarters Services, Directorate for Information Operations and Reports, 1215 Jefferson Davis Highway, Suite 1204, Arlington, VA 22202-4302, and to the Office of Management and Budget, Paperwork Reduction Project (0704-0188) Washington DC 20503.

1. AGENCY USE ONLY (Leave blank)	2. REPORT DATE	3. REPORT TYPE AND DATES COVERED
	December 1995	Engineer's Thesis
4. TITLE AND SUBTITLE ORBITAL PERTURBATION ANALYSIS OF EARTH-CROSSING ASTEROIDS		5. FUNDING NUMBERS
6. AUTHOR(S) Knudson, Wade E.		
7. PERFORMING ORGANIZATION NAME(S) AND ADDRESS(ES) Naval Postgraduate School Monterey CA 93943-5000		8. PERFORMING ORGANIZATION REPORT NUMBER
9. SPONSORING/MONITORING AGENCY NAME(S) AND ADDRESS(ES) Space Warfare Center, Falcon AFB, Colorado		10. SPONSORING/MONITORING AGENCY REPORT NUMBER
11. SUPPLEMENTARY NOTES The views expressed in this thesis are those of the author and do not reflect the official policy or position of the Department of Defense or the U. S. Government.		
12a. DISTRIBUTION/AVAILABILITY STATEMENT Approved for public release; distribution is unlimited.		12b. DISTRIBUTION CODE

13. ABSTRACT (maximum 200 words)

Earth-Crossing Asteroids (ECAs) are those asteroids whose orbit cross-section can intersect the capture cross section of the Earth as a result of secular gravitational perturbations. This thesis provides a framework for understanding the origin, nature, and types of ECAs. The change in velocity requirements to achieve a two Earth radii deflection for long and short-term warning scenarios are developed. Next, a method of developing hypothetical Earth colliding asteroid orbits is presented. These hypothetical orbits are used in two ways: (1) to evaluate the ability of *Dance of the Planets*, a solar system simulation model developed by Applied Research and Consulting, Inc., to accurately propagate orbits of imported asteroid orbits, and (2) to analyze the sensitivity of deflection distance to variation in deflection angle and orbital parameters of a given orbit. Inaccuracies during importation of data precluded the use of *Dance of the Planets* for the purpose of sensitivity analysis. The program does provide an excellent tool for visualization of ECA scenarios. Consequently, a simpler orbital model was developed to provide a Earth miss distance sensitivity analysis. With one asteroid orbital period warning the minimum change in velocity to deflect an asteroid two Earth radii is approximately 0.135 m/s and the optimal deflection is along the flight path. Maximum deflection occurs when the deflection is applied at perihelion. The miss distance decreases markedly with increase in true anomaly until it is a minimum at aphelion.

14. SUBJECT TERMS Earth-crossing Asteroid, Perturbation, Near Earth Object, Mitigation, Asteroid, Aten, Apollo, Amor, Comet			15. NUMBER OF PAGES 111
			16. PRICE CODE
17. SECURITY CLASSIFICATION OF REPORT Unclassified	18. SECURITY CLASSIFICATION OF THIS PAGE Unclassified	19. SECURITY CLASSIFICATION OF ABSTRACT Unclassified	20. LIMITATION OF ABSTRACT UL

Approved for public release; distribution is unlimited.

ORBITAL PERTURBATION ANALYSIS OF EARTH-CROSSING ASTEROIDS

Wade E. Knudson

Lieutenant Commander, United States Navy
B.S., United States Naval Academy, 1984

Submitted in partial fulfillment of the
requirements for the degree of

AERONAUTICAL AND ASTRONAUTICAL ENGINEER

from the

NAVAL POSTGRADUATE SCHOOL
December 1995

Author: WE Knudson

Wade E. Knudson

Approved by: I. M. Ross

I. M. Ross, Thesis Advisor

K. T. Alfriend

K. T. Alfriend, Second Reader

Daniel J. Collins

Daniel J. Collins, Chairman

Department of Aeronautical and Astronautical Engineering

ABSTRACT

Earth-Crossing Asteroids (ECAs) are those asteroids whose orbit cross-section can intersect the capture cross section of the Earth as a result of secular gravitational perturbations. This thesis provides a framework for understanding the origin, nature, and types of ECAs. The change in velocity requirements to achieve a two Earth radii deflection for long and short-term warning scenarios are developed. Next, a method of developing hypothetical Earth colliding asteroid orbits is presented. These hypothetical orbits are used in two ways: (1) to evaluate the ability of *Dance of the Planets*, a solar system simulation model developed by Applied Research and Consulting, Inc., to accurately propagate orbits of imported asteroid orbits, and (2) to analyze the sensitivity of deflection distance to variation in deflection angle and orbital parameters of a given orbit. Inaccuracies during importation of data precluded the use of *Dance of the Planets* for the purpose of sensitivity analysis. The program does provide an excellent tool for visualization of ECA scenarios. Consequently, a simpler orbital model was developed to provide a Earth miss distance sensitivity analysis. With one asteroid orbital period warning the minimum change in velocity to deflect an asteroid two Earth radii is approximately 0.135 m/s and the optimal deflection is along the flight path. Maximum deflection occurs when the deflection is applied at perihelion. The miss distance decreases markedly with increase in true anomaly until it is a minimum at aphelion.

TABLE OF CONTENTS

I. INTRODUCTION.....	1
II. NEAR EARTH OBJECTS	5
A. INTRODUCTION.....	5
B. ASTEROIDS	5
1. Early History	7
2. Origin and Nature of Asteroids.....	8
3. Asteroid Close Approaches.....	9
4. Earth-Crossing Asteroids	10
C. COMETS.....	20
1. Comet Classifications	21
2. The Origin and Nature of Comets.....	22
3. The Oort Cloud	22
4. The Kuiper Belt.....	23
III. DEFENDING THE EARTH AGAINST IMPACTS FROM LARGE COMETS AND ASTEROIDS.....	25
A. INTRODUCTION.....	25
B. DEFLECTION CONSIDERATIONS	28
1. Size Limitations	28
2. Directional Considerations.....	30
IV. DEVELOPMENT OF HYPOTHETICAL ORBITS.....	37
A. INTRODUCTION.....	37
B. COORDINATE SYSTEMS	37
1. Heliocentric Ecliptic Coordinate System	38
2. Perifocal Coordinate System.....	38
C. CLASSICAL ORBITAL ELEMENTS	39
D. DERIVATION OF FORMULAE	40
1. Procedure	40
2. Determination of r and v From Intersecting Orbit Parameters.....	46
3. Orbit Rotations.....	47
V. CASE STUDIES.....	49
A. INTRODUCTION.....	49
B. DANCE OF THE PLANETS.....	50
1. Hypothetical Orbit Determination	50

V. CASE STUDIES.....	49
A. INTRODUCTION	49
B. DANCE OF THE PLANETS	50
1. Hypothetical Orbit Determination.....	50
2. Initialization	51
3. Constants	52
4. Orbital Element Selection	53
5. Asteroid Orbit Rotations.....	54
6. Simulation	55
7. Results and Discussion.....	56
C. DEFLECTION RATIO SENSITIVITY TO ORBITAL PARAMETERS	58
1. Introduction	58
2. Variation in Orbital Period for a Circular Orbit	59
3. Constant Radius of Perihelion.....	60
4. Variation in Eccentricity	61
5. Conclusions.....	62
VI. CONCLUSIONS AND RECOMMENDATIONS.....	63
A. SUMMARY.....	63
B. FURTHER RESEARCH OPPORTUNITIES	64
LIST OF REFERENCES	65
APPENDIX: MATLAB SCRIPT FILES	67
INITIAL DISTRIBUTION LIST	99

ACKNOWLEDGMENTS

I would like to acknowledge the financial support of Space Warfare Center, Code DOZ, Falcon AFB for providing the funds to purchase equipment used in this thesis. I would also like to extend my appreciation to Prof. I. M. Ross and Prof. K. T. Alfriend for their guidance and patience during the work in completing this thesis.

I. INTRODUCTION

Impacts by Earth-crossing Asteroids (ECAs) and comets, collectively known as Near-Earth Objects (NEOs), pose a significant and unique challenge to the scientific community. The study of these space-borne bodies has spanned a broad range of disciplines: mechanical, electrical, aeronautical, and astronautical engineers, astronomers, nuclear physicists, to name but a few. Various camps have, at different times, proposed new search strategies and detection methods to ensure a proper tally of potential colliders, forwarded techniques, both nuclear and non-nuclear, to mitigate the disaster a colliding body may impart, and designed missions to intercept, rendezvous, and study a few of the closer bodies. The recent impact of comet Shoemaker-Levy 9 with Jupiter only served to stimulate additional interest in the subject of NEOs.

Recognizing the potential seriousness of such events, the United States Congress in 1992 mandated that the National Aeronautics and Space Administration (NASA) conduct two workshops to study two major research areas of NEOs: Detection and Mitigation. The United States House of Representatives, in NASA Multiyear Authorization Act of 1990 said, in part:

The committee believes that it is imperative that the detection rate of Earth-orbit-crossing asteroids must be increased substantially, and that the means to destroy or alter the orbits of asteroids when they threaten collision should be defined and agreed upon internationally.

The chances of the Earth being struck by a large asteroid are extremely small, but since the consequences of such a collision are extremely large, the Committee believes it is only prudent to assess the nature of the threat and prepare to deal with it. We have the technology to detect such asteroids and to prevent their collision.

The Committee therefore directs that NASA undertake two workshop studies. The first would define a program for dramatically increasing the detection rate of Earth-orbit-crossing asteroids; this study would address the costs, schedule technology, and equipment required for precise definition of the orbits of such bodies. The second study would define systems and technologies to alter the orbits of such asteroids or to destroy them if they should pose a danger to life on Earth. The Committee

recommends international participation in these studies and suggest that they be conducted within a year of the passage of this legislation. [Ref. 1]

As a result two conferences were conducted. The first, the NASA International Near-Earth-Object Detection Workshop, was conducted in three sessions from June through November 1991. Their work concentrated on improving the rate at which ECAs are discovered; the results are documented in reference 1. The second conference, The Near-Earth-Object Interception Workshop, was held in January 1992 and hosted by Los Alamos National Laboratory. It concentrated on the issues surround the mitigation of ECAs and associated technologies. Even more recently, an ECA conference was held in March 1995 at Lawrence Livermore National Laboratories. Conference proceedings have not yet been published.

These conference reports address the majority of the issues surrounding NEOs; however, there is much work remaining. Advances in detection technology such as improved sensors, computer search algorithms, and space radar support would significantly speed the rate at which NEOs are identified. Space missions to candidate asteroids can provide essential information regarding the structure and composition of asteroid bodies. Optimization of intercept trajectories and continued improvements to the space launch vehicles will all be directly applicable to the mitigation of these potentially dangerous objects.

At the onset of this project there were three main goals: (1) Conduct a thorough and exhaustive survey of the current literature in the area of ECAs, (2) Analyze and select from commercially available software applications the candidate most likely to aid in the visualization of asteroid mitigation through deflection, and (3) Develop mitigation scenarios and determine the sensitivity of the circular solution to elliptical orbits.

Research under the Space Warfare Research Program, sponsored by the Air Force's Space Warfare Center, was divided into four sections. Two major components of NEOs, ECA's and Earth-crossing Comets (ECCs), are described and categorized.

Deflection options are presented and the maximum size asteroid which could be deflected is estimated. The most effective deflection angle is established and the required change in velocity to perturb an object by two Earth radii is determined. Methodology for developing hypothetical asteroid orbits is also presented. A commercially available software application, *Dance of the Planets*, is evaluated for its usefulness in verifying the deflection of assailant objects and testing the mathematical solutions for optimal deflection. Finally, an analysis of sensitivity of miss distance to variations in orbit shape and deflection direction is conducted. The issues compiled in this thesis address only a small portion of the asteroid mitigation problem, and an even smaller portion of the broader subject of ECAs.

II. NEAR EARTH OBJECTS

A. INTRODUCTION

There are two broad categories of objects whose orbits bring them close to that of the Earth: asteroids and comets. Astronomers classify the objects into one of the two categories based upon their telescopic appearance. Any object which appears to be star-like is called an asteroid. If the object has a visible atmosphere or a tail then it is a comet. [Ref. 1] This difference is, in part, due to the composition of the object. Asteroids have no atmosphere and may have physical and compositional properties ranging from loosely aggregated cometary ices to solid metal. [Ref. 2] Comet nuclei are composed of a complex mixture of volatile ices, water, and hydrocarbon and silicate grains. As a comet is heated by the Sun as it approaches perihelion, there is a noticeable out-gassing of evaporative material. [Ref. 3] Further discussions on each broad classification of Near-Earth Objects (NEOs) are provided below.

B. ASTEROIDS

When viewing the solar system, shown in Figure 1Figure 1, the empty gap between Mars and Jupiter is readily apparent. Kepler contemplated a “missing planet” as he studied the solar system, as described by the measurements of Tycho Brahe. [Ref. 4]

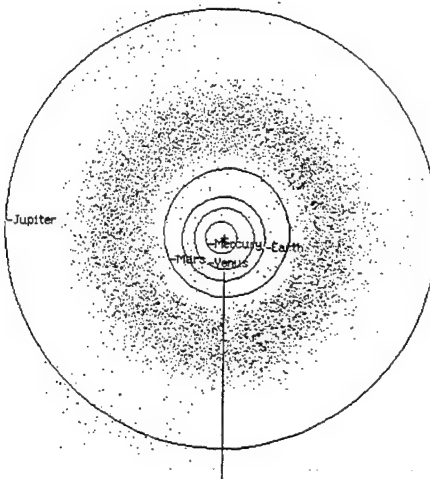


Figure 1. Depiction of Solar System Through Jupiter. From Ref. 4.

Bode's law, named after Johann Bode's effort to stir interest in an unknown planet in 1772, uses a simple relationship to generate the mean distances in Astronomical Units (AU) of the principal planets. The relationship is generated by writing down the series 0, 3, 6, 12, ..., add 4 to each number and dividing by 10. As shown in Table 1, Bode's law generates fairly accurate locations for all the planets except Neptune and Pluto.

PLANET	BODE'S LAW DISTANCE	ACTUAL DISTANCE
Mercury	0.4	0.39
Venus	0.7	0.72
Earth	1.0	1.00
Mars	1.6	1.52
Asteroids (average)	2.8	2.65
Jupiter	5.2	5.20
Saturn	10.0	9.52
Uranus	19.6	19.28
Neptune	38.8	30.17
Pluto	77.2	39.76

Table 1. Bode's Law vs. Mean Planetary Distance

This fits the actual positions of the planets through Saturn very well, except for the position at 2.8 AU. This position, between the orbit of Mars and Jupiter remains empty, except for the asteroid belt. [Ref. 4]

1. Early History

In view of Bode's law, a group of 24 astronomers formed a society in Europe in 1800 to solve the problem of a planet, surmised to be missing, between Mars and Jupiter. Each astronomer was given a region of the zodiac. [Ref. 4].

Giuseppe Piazzi, in Palermo, Italy, was already engaged in a star charting project. He located a dim, uncharted 'star' that shifted position from night to night. This was Ceres, discovered on January 01, 1801. He observed it for 41 days before it was lost due to bad weather and the illness of Piazzi. [Ref. 4].

Karl Friedrich Gauss became involved with the intricate mathematical problem of calculating an adequate recovery orbit for Ceres. With his help, Ceres was sighted on December 07, 1801. Gauss' ingenuity was of great significance to the field of celestial mechanics. The basic elements of Ceres were eccentricity of 0.08, inclination of 11°, and semi-major axis of 2.77 AU. [Ref. 4].

Heinrich Wilhelm Olbers found a second unknown 'planet', Pallas, in March 1802, while helping Gauss observe Ceres. Gauss next calculated an orbit for Pallas. Many scientists contributed in the calculation of the orbital elements, and in the development of perturbation theories to account for the influence of Jupiter. This was one of the first documented efforts at the development of planetary theory from which highly accurate planet ephemerides are possible. [Ref. 4].

Discovery of additional asteroids progressed rapidly over the course of the next century, particularly with the implementation of photography in the search process in 1891. By 1900, 463 asteroids had been discovered, and by 1950, 1568. By 1993, approximately 5500 numbered asteroids had been documented. Approximately 300

numbered asteroids are added annually. Numbered asteroids have orbits confirmed by observations at two or more oppositions (when the asteroid-Earth-Sun angle equals 180°). Many others asteroids have only provisional designations. [Ref. 4].

2. Origin and Nature of Asteroids

There are many plausible explanations for the existence and formation of asteroids. One scenario suggests the asteroids formed from planetesimals which were never able to accrete into planet sized bodies due to the disturbing influences of a proto-Jupiter. There are many inconsistencies with this theory. First, from the planetesimal model, there should be between one and two Earth masses of planetesimals in the region of the asteroid belt. All of the asteroids together, however, are no more than 0.08% of the mass of the Earth. Some mechanism is responsible for this loss of mass. Secondly, individual asteroids have high relative velocities. They do not fit the orderly picture of planetesimals analogous to Saturn's rings: bodies lying in nearly the same plane with low relative velocities between neighboring bodies. Again, some mechanism is responsible for the high relative velocities which produce collision fragmentation and not collision-accretion. Finally, many stony and metallic meteorites, derived from asteroids, have clear indications of melting, elemental differentiation, and slow cooling, similar to that found in the planets. The process of this development is not fully understood. [Ref. 4].

There has been much debate as to the origin of near-Earth asteroids. Because these are planet crossing asteroids, they have a dynamic lifetime (the average time before a planet crossing asteroid impacts one of the inner planets) of approximately 3×10^7 yr. As such, there must be some mechanism responsible for their replenishment. There are two main theories, divided largely between observers and dynamicists, which attempt to explain the source of these objects. Observers generally believe that the near-Earth asteroids were derived from the main asteroid belt due to spectropically similar objects in the main belt. Dynamicists believe they may be largely of cometary origin. They do not

believe that there is sufficient dynamical interaction in the main asteroid belt to resupply the near-Earth orbit asteroid population. [Ref. 3]

Asteroids are numbered in the order they are discovered with orbits verified with a minimum of three observations. The majority also have names assigned. The first asteroid discovered, 1 Ceres, is approximately 932 km in diameter, and represents about 30% of the total mass of asteroids. 4 Vesta and 2 Pallas, approximately 528 km and 523 km, respectively, are next in size. There are approximately 30 other main belt asteroids with diameters larger than 200 km. For objects with the same density, the mass varies as the third power of their linear dimensions. From this, it is easy to ascertain that most of the total mass of the asteroids is found in the few largest. Ceres is just below the limit for the class-3 satellite size category of 1000–1600 km, of which Saturn and Uranus each have four. [Ref. 4].

3. Asteroid Close Approaches

Although there are a large number of asteroids, their number is limited by our ability to detect them. This remains one of the biggest challenges in the field. Most newly discovered asteroids are dimmer and usually smaller than previously discovered asteroids. By far the majority are fragments of ancient parent bodies, unlike Ceres which has retained most of its original shape and mass. [Ref. 4].

Near Earth Asteroids (NEA) are of interest because they lie well inside the main asteroid belt, and they do not have long term stability because they will eventually either 1) collide with one of the inner planets, or 2) be ejected from this region by a near-collision encounter. Earth impact rate for objects of potentially cataclysmic size is estimated at 3-4 per million years. No such collisions have been yet been predicted, however. The “spacewatch” telescope on Kitt Peak finds several close approaches per month. [Ref. 4].

Many ECAs have come relatively close to the Earth. Hermes, in 1937, passed within 800,000 km (twice the distance to the Moon) of the Earth. Its orbit was lost and its location is no longer known. On January 18, 1991, 1991BA passed within approximately 170,000 km (0.0011 AU) of the Earth. The newly discovered near-Earth asteroid 1994 XM1 made the closest approach to the Earth of any object discovered outside the earth's atmosphere---some 105,000 km on the morning of Dec. 9 over Russia. The diameter was estimated to be approximately 6-13 meters.

There are many more asteroids with the potential for inner planet encounters. Among them are 433 Eros, 887 Alinda, 1036 Ganymed, 1221 Amor, 1566 Icarus, 1580 Betulia, 1620 Geographos, and 1627 Ivar. There are many other inner asteroids of note. 3200 Phaethon has the greatest asteroid eccentricity, and the smallest perihelion, 0.135 AU, 1951 Lick is located entirely between the orbits of Earth and Mars; it doesn't cross any orbit. 2062 Aten is entirely inside Earth's orbit. 2102 Tantalus has the highest inclination of any numbered asteroid (64°). 1973na has an even greater inclination (68°).

4. Earth-Crossing Asteroids

There are many asteroids well within the orbits of the inner planets. A current list of all ECAs through 1991 is contained in reference 5. These asteroids are of interest because they lie well inside the main asteroid belt. Some of these come quite close to the orbit of Earth. An Earth-crossing Asteroid (ECA) has been defined as a minor planet whose orbit can intersect the capture cross-section of the Earth as a result of secular gravitational perturbations. [Ref. 5] ECAs have secular periods on the order of tens of thousands of years.

a. Secular Variations

It has been shown that an asteroid orbit which overlaps the orbit of a planet may, as a result of the advance of the line of apsides, intersect the orbit of the planet. If

the orbit of the planet is of low eccentricity and is overlapped by an asteroid orbit which is highly eccentric, the two orbits will be linked, like links of a chain, when the argument of perihelion is 0 or π and unlinked when the unlinked at $\pi/2$ or $3\pi/2$. In one complete rotation of the line of apsides, the orbits transition from linked to unlinked states a total of four times, providing four possible intersections of the two orbits. These intersections of crossings may be found by solving the polar equation of the ellipse, and occur at

$$\omega = \cos^{-1} \pm \frac{1}{e} \left[\frac{a(1-e^2)}{\rho} - 1 \right] \quad (1)$$

where ω is the argument of perihelion, a is the semi-major axis of the asteroid orbit, e is the eccentricity of asteroid orbit at the time of intersection, and ρ is the radius to the planet's orbit along the line of nodes at the time of intersection. [Ref. 6] Because most planet's orbits are not circular and there are secular variations in e , ρ will have four different values for each rotation of the line of apsides which can be found by simultaneously solving Eqn (1) and the polar equation for the elliptical orbit of the planet. This type of orbit is referred to as a *quadruple crosser*, and is shown in Figure 2 using asteroid 2062 Aten as an example. The figure shows one cycle of advance of ω starting at $\omega = 0$. The solid line shows the ascending node and the dashed line shows the descending node.

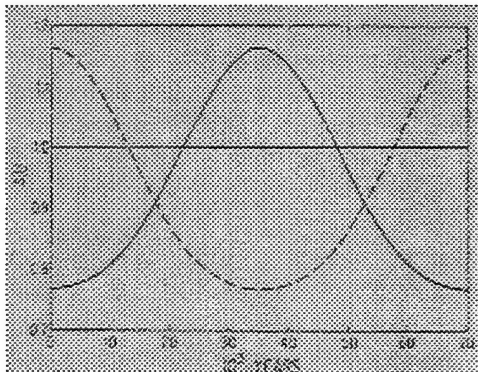


Figure 2. Secular Variation of Radius to the Node of the Orbit of 2062 Aten. From Ref. 6.

Secular variations in e may be sufficiently high to change the depth of orbital penetration of the assailant body. In this case the orbits may transition from a non-overlapped condition at $\omega = 0, \pi$ to a relatively deep overlap at $\omega\pi/2, 3\pi/2$. The first crossing occurs due to the secular increase in e as ω begins its rotation from 0 to $\pi/2$, thus linking the orbits. The second crossing occurs as ω increases sufficiently to unlink the orbits. Thus, there are two crossings during each $1/2$ advance of the line of apsides. This type of asteroid is known as an *octupole crosser*. An example is shown in using asteroid 1580 Betulia, the first asteroid where this type of behavior was recognized. [Ref. 6] Approximately 1.5 cycles of advance of ω are shown, with the solid line representing the ascending node and the dashed line representing the descending node.

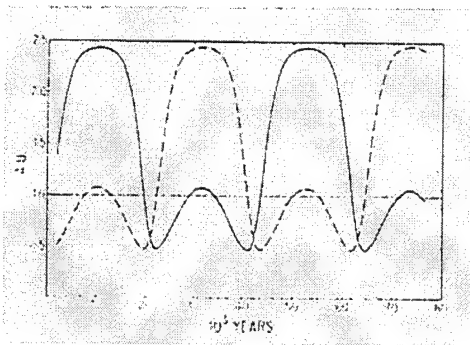


Figure 3. Secular Variation of Radius to the Node of the Orbit of 1974MA. From Ref. 6.

If the inclination of the asteroid with respect to the ecliptic plane is sufficiently high, the secular perturbations are not strong enough to influence a continuous advance in ω . In this case, ω librates around $\pi/2$ or $3\pi/2$. When this occurs, a large oscillation of e can occur during the libration cycle leading to orbit intersection four times during each libration cycle of ω . These types of asteroid are called *quadruple crossing omega librators*. An example is shown in Figure 4 using asteroid 1973 NA. Approximately five libration cycles of omega are shown. [Ref. 6].

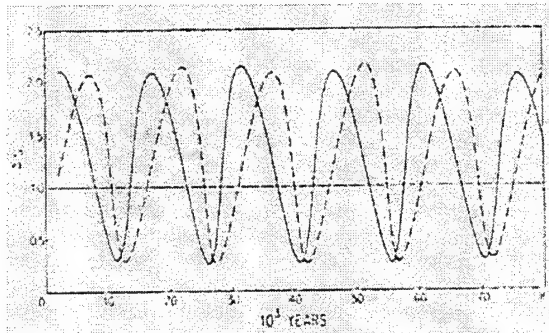


Figure 4. Secular Variation of Radius to the Node of the Orbit of 1973 NA. From Ref. 6.

The fourth type of ECA are known as *supercrossers* and result from asteroids that librate about the 3:1 commensurability with Jupiter. The resonant effects of these perturbations cause a relatively high frequency oscillation in a and e which lead to relatively high frequency oscillations (4 cycles in approximately 1400 years) between periods of overlap and nonoverlap of the two orbits. For example, asteroid 1915 Quetzalcoatl, shown in Figure 5, had nine crossings of the Earth's orbit over a period of approximately 1400 years. Approximately four cycles of libration of the mean motion of the asteroid are shown. [Ref. 6].

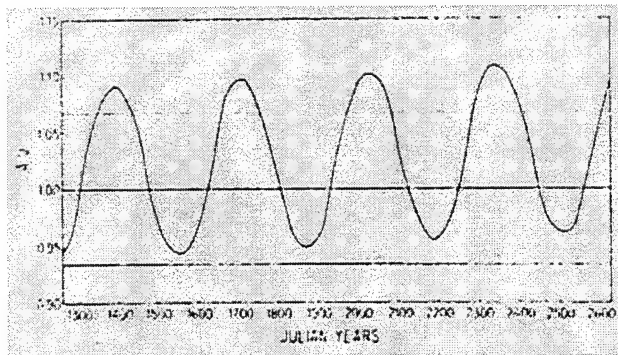


Figure 5. Secular Variation of Radius to the Ascending Node of 1915 Quetzalcoatl. From Ref. 6.

b. *Classes of Earth-Crossing Asteroids*

In addition to classifying asteroids by the type of secular perturbations they experience, Earth-crossing asteroids are further divided into three groups on the basis of

their present osculating orbital elements: (1) Aten asteroids, (2) Apollo asteroids, and (3) Earth-crossing Amor asteroids.

(1) Aten. The orbits of Aten asteroids have a semi-major axis less than 1 AU. Their orbits overlap those of the Earth near their aphelia, as shown in Figure 6.

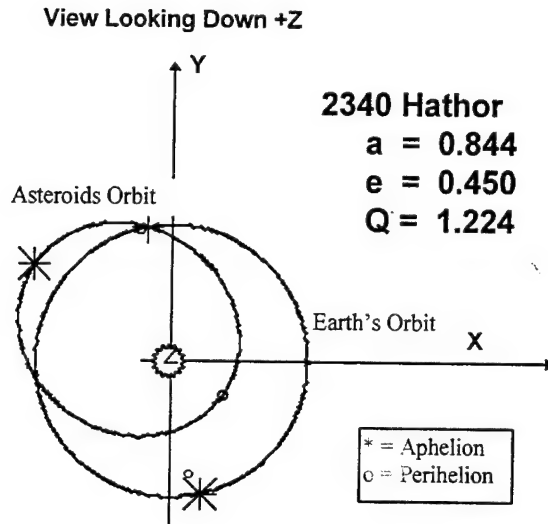


Figure 6. An Aten Type Asteroid.

This class includes all asteroids with $a < 1.0$ AU and with the aphelion distance of the asteroid, $Q > 0.983$ AU. The asteroid's orbit can intersect that of Earth as the Earth's perihelion distance is 0.983 AU. The first Aten was discovered relatively recently, in 1976. Fifteen were known as of August 1993. They represent approximately 10% of the 180 known ECAs. The first three discovered exhibit continuous, or nearly continuous orbital overlap with Earth and are characterized as deep quadruple crossers. [Ref. 6].

The total number of Aten asteroids to visual magnitude has been estimated to be on the order of 100. In the same way that some Earth-crossing Amors have current osculating orbits entirely outside the orbit of the Earth, some Atens may have orbits entirely inside the orbit of the Earth. Shoemaker et. al. numbers these at a few tens of objects out to visual magnitude 18. [Ref. 6]

(2) Apollo. The orbits of Apollo asteroids are those asteroids with $a \geq 1.0$ AU, and perihelion distance, $q \leq 1.017$ AU, where 1.017 is the aphelion distance of the Earth. An example is presented in Figure 7.

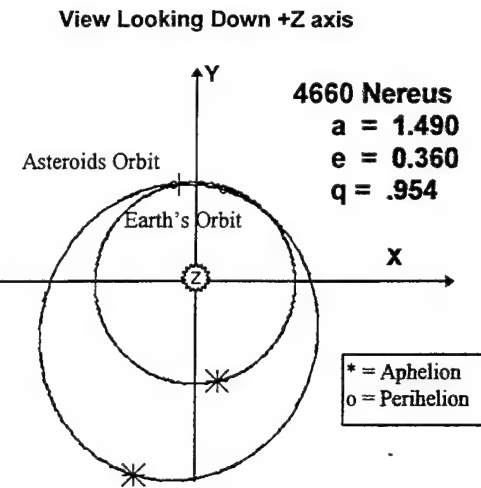


Figure 7. An Apollo Type Asteroid.

125 Apollos have been discovered, which represents approximately two-thirds of all ECAs. All but about 5% of all Apollo asteroids are ECAs. [Refs. 6 and 5] Of those known in 1979, approximately 60% were quadruple crossers, 20% were octuple crossers, 5% were quadruple crossers part of the time at octuple crossers part of the time, and 15% were quadruple crossing ω librators. [Ref. 6] In 1932 the first Earth-crossing asteroid, 1862 Apollo, was found by K. Reinmuth at Heidelberg. [Ref. 8]

(3) Amor. Although Amor asteroids have perhaps the simplest definition of all, the fact that some are in Earth-crossing orbits can be confusing. Their orbits are defined strictly upon the orbital perihelion distance, $1.017 \leq q \leq 1.3$ AU. They have perihelions close, but a little outside of the Earth's orbit. The first discovery of an asteroid of this class was 433 Eros in 1898. [Ref. 4] However, the traditional name for Atens comes from the asteroid of the same name discovered by E. Delporte at Uccle, in 1932. [Ref. 8] The 47 known Amor asteroids comprise approximately 25% of all ECAs. [Ref. 5] The upper limit for perihelion distance of 1.3 AU was chosen because it is

near a minimum in the radial frequency distribution of q for discovered objects. [Ref. 6] As discussed previously, some Amors can become Apollos and vice versa, due to secular perturbations. The classifications are based on the category at the time of discovery. For example, if the Amor asteroid 1915 Quetzalcoatl had been discovered in 1942, it would have been classified as an Apollo asteroid. [Ref. 6] An example of an Earth-crossing Amor is shown Figure 8.

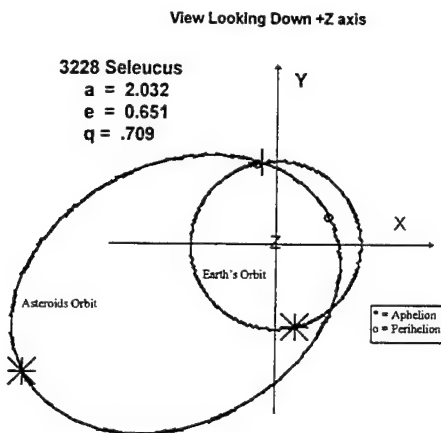


Figure 8. An Amor Type Asteroid.

c. *Distant Asteroids*

While most asteroids are contained within the main belt, there are some that lie outside that area. The Trojans, shown in Figure 1, are a group of approximately 100 asteroids in two thinly populated lobes centered on Jupiter's orbit at about the Lagrangian L_4 and L_5 points. They are in stable orbits and have an orbital resonance of 1:1 (the ratio of the number of orbits of the asteroid to that of a third body) with Jupiter. While not tightly grouped about the Lagrangian points, they librate about these nominal positions, moving closer and further from Jupiter, but not far from its orbit. [Ref. 4]

Opposite Jupiter, there is a thinner lobe centered on the Lagrangian L₃ point. These are known as the Hilda asteroids and have a 3:2 resonance with Jupiter. Over 40 Hilda type asteroids have been discovered. Hilda orbits are very similar to some short-period comet orbits. The difference being that the Hilda asteroids are in stable orbits while the short-period comets are not. [Ref. 4]

Another asteroid of note is 279 Thule. It is the only known 4:3 asteroid. It is unique in that having a resonance near unity places it near Jupiter's orbit where it is strongly perturbed every three Jovian years, yet remains in a stable orbit. 944 Hidalgo has a comet-like orbit that takes it out nearly to Saturn. 1373 Cincinnati experiences relatively strong perturbations from Jupiter but has no resonance making it unique.

2060 Chiron was the first trans-Saturn asteroid. Discovered in 1977, it has a diameter of approximately 200 km. Its motion has been simulated by researchers back to 1664 BC, when it appears to have come within approximately 0.1 AU of Saturn. 1992QB1 appears to be of similar size to Chiron but its orbit extends beyond that of Pluto. Exotic bodies such as these may be from the long-postulated Kuiper belt, discussed in the comet section.

d. Asteroid Classifications

Asteroids are of four different classifications based upon the photometric characteristics of the reflected light, the amount of which is a function of their nature and composition of their surface material. This classification is only based upon spectral characteristics. The main types have good correlation to location in the asteroid belt. Most asteroids fall into one of the following four categories. [Ref. 4].

S-type. A broad distribution of asteroids centered at about 2.3 AU from the Sun. This type is associated with stony-iron meteorites, although some scientists question this association. These asteroids have high concentrations of nickel and iron, with approximately equal amounts of metals and silicates. These are presumed to be the

exposed fragments from the inner cores of larger parent bodies. These are the second most prevalent type of asteroid. [Ref. 4].

C-type. The most common type of asteroid with a relatively sharp distribution centered at about 3.1 AU from the Sun. Thought to be composed of material similar to carbonaceous chondritic meteorites, C-types are very dark with an albedo of approximately 0.04. They have various grainy, carbon rich, rock-like mineralogies, and are a complicated group to examine photospectrally. Most scientists agree Ceres is a C-type asteroid. [Ref. 4].

M-type. Asteroids with moderate reflectivity and a reddish spectra associated with metals, particularly Ni-Fe are known as M-type asteroids. Similar meteorites are the nickel-irons and the enstatite chondrites, which have Ni-Fe embedded in silicates. There are not many M-type asteroids. The distinction between M-type and S-type asteroids is not clear and there are many similarities between them. [Ref. 4].

D-type. D-type asteroids have low albedos and reddish spectra and are primarily the Trojans, located near the orbit of Jupiter. They are composed mostly of clays with magnetite and carbon-rich materials. No meteorites match these spectral characteristics but the dark side of Saturn's Iapetus is a good match. [Ref. 4].

e. Earth-Crossing Asteroid Population

Visual magnitude is defined as an arbitrary number, measured on a logarithmic scale, used to indicate the brightness of an object. A one magnitude difference is the fifth root of 100, and is approximately equal to a factor of 2.512. The brighter the asteroid, the lower the numerical value of magnitude. Very bright objects have negative magnitudes.

The absolute magnitude, H , of an asteroid is the magnitude the asteroid would have if it were 1 AU from the Sun, and viewed from the Sun. For example, if an

asteroid was 2 AU from the Sun and viewed from 1 AU away, it would be four times dimmer, or about 1.5 magnitude less bright.

As most ECAs are discovered through direct telescopic observation, the absolute magnitude of the asteroids is of extreme importance to an observer. In general, the larger the diameter of an object, the lower the value of absolute magnitude (the object is brighter than a similar asteroid of smaller diameter). As a result, the large asteroids are often discovered more quickly than the smaller objects.

The two most common types of asteroids are C-type and S-type. Table 2 presents the current estimates of ECA discovery completeness based on absolute magnitude, H. Estimated diameters, based on the albedo of the two most prevalent types of asteroids, are also presented.

H	Percent discovered	Asteroid type	
		C-type diameter	S-type diameter
13.2	100%	12 km	6 km
15.0	35%	6 km	3 km
16.0	15%	4 km	2 km
17.7	7%	2 km	1 km

Table 2. Estimated Discovery Completeness From Ref. 5

Numerous studies have attempted to estimate the total number of asteroids in Earth-crossing orbits. These estimates are based on a power law relationship

$$N = k D^b \quad (2)$$

where N is the number of asteroids larger than a given diameter, D. k is a constant and b is the power-law exponent. The general form of the size distribution is based on observation as the actual detailed distributions remain unknown.

There are approximately 180 known Earth-crossing asteroids. The characteristics of Apollo asteroids that overlap the Earth's orbit part of the time and the characteristics of Earth-crossing Amors are essentially identical. The distinction is

derived from the present state of the cycle of variation of their perihelion distance. The majority of Earth-crossing Amors are shallow crossers, while the majority of Apollos are deep crossers. Because the orbits of most Earth-crossing Amors only overlap the orbit of Earth for a small period of time, they retain their traditional classification as Amor asteroids. [Ref. 6]

Based on the best information to date, an estimate of the number of Earth-crossing asteroids larger than a given diameter, D , are shown in Figure 9. For this population model, changes in the power law are estimated to occur at diameters of 10 m, 70 m, and 3.5 km.

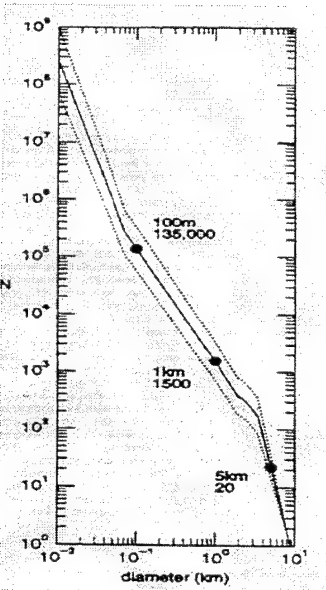


Figure 9. Estimated Number of Earth-Crossing Asteroids. From Ref. 5.

C. COMETS

Comets are a diffuse bodies of gas and solid particles (such as CN, C₂, NH₃, and OH), which orbit the Sun. Their orbits are highly elliptical or even parabolic in nature. Edmund Halley used Newton's celestial mechanics to show that comets orbited the Sun. He then deduced that one spectacular comet in particular was returning to Earth with a period of 76 years. His correct prediction of the comet's return in 1758 made it comet

Halley. Today, as many as 10^{11} to 10^{12} comets remain, orbiting the solar system in the Oort Cloud and Kuiper Belt, described in Section 2, below.

1. Comet Classifications

Comets which have an elliptical orbit are known as periodic comets. A significant number of comets also have parabolic or hyperbolic orbits and will, therefore, make only one perihelion passage. The periodic comets are further divided into short-period and long-period comets.

a. *Short-Period Comets*

Short period comets are defined as those whose orbits lie predominately within the realm of the solar system. These include all the comets which have been seen more than once. The shortest known period is that of comet Encke at 3.3 years while the longest extend up to 200 years. Most short-period comets have inclinations close to the ecliptic, less than approximately 35° . [Refs. 4 and 3] About 95% move in a direct sense. Comet Halley is a short period comet in a retrograde orbit. More recently, short-period comets have been further divided into two additional classes: (1) Jupiter and (2) Halley. Comets in the Jupiter family have periods of less than 20 years with inclinations close to that of the ecliptic and direct orbits. Halley type comets have period of $20 < P < 200$ years. In general, Halley type comets have higher average inclinations than Jupiter type comets.

b. *Long-Period Comets*

Long period comets are those with periods greater than 200 years. Long-period comets are randomly distributed on the celestial sphere. Often it is difficult to distinguish an orbit with a very long period (on the order of 10^5 - 10^7 years) from a parabolic or hyperbolic orbit. Many appear to have aphelia of 20,000-50,000 AU. These types of comets come from all directions. There is no relationship for the orientation of

the orbit with respect to the ecliptic or for direct revolution. Approximately one-third of all long-period comets observed are on weakly hyperbolic orbits.

2. The Origin and Nature of Comets

Many scientists believe comets to be planetesimals formed in the colder reaches of the solar system, beyond Saturn, and perhaps beyond Neptune. Those “cometesimals” in the planet realm of the solar system were presumed to be ejected by perturbations from the outer planets. These comets now reside in the Oort Cloud, at the outer reaches of our Sun’s gravitational influence. The Oort cloud, named after Jan Oort in 1950, is a reservoir of comets located about a light-year from the Sun.

Comets are brought into the Earth’s realm from their orbits in the Oort cloud or the Kuiper belt as they are perturbed by Jupiter or passing stars every few million years and result in comet insertion back into the solar system. [Ref. 9]

At the same time Jan Oort was formulating his hypothesis, the structure of comets was proposed by Fred Whipple. His “dirty snowball” model hypothesizes a composition of various ices, predominantly H₂O, along with lesser amounts of silicate and other mineral dusts. This analysis of the dirty snowball/Oort cloud has remained the generally accepted model, with subsequent modification and elaboration due to follow-on research. Relatively recent comet space probes, particularly to comet Halley in 1986, have greatly increased general knowledge about the comet.

3. The Oort Cloud

The factors that led to Oort’s comet cloud model were 1) very long-period orbits that were commonly found to have aphelia of around 50,000 AU, 2) the large reservoir that would be required in order to supply comets over the last 4 billion years at the rate they appear in the inner solar system (a trillion or so), and 3) the fact that very long-period comets appear from all directions. Oort proposed that the planetary system was

surrounded by a distant spherical cloud of comets extending approximately one-half the distance to the nearest stars. The comet cloud is perturbed by passing stars which cause the injection of a long-period comet into our solar system. The source of the Oort cloud is postulated to be icy planetesimals ejected by the proto-planets in the outer solar system, particularly Uranus and Neptune. [Ref. 3]

4. The Kuiper Belt

The Kuiper Belt is a disk thought to be composed icy planetesimal remnants beyond Neptune, and was first proposed by Kuiper in 1951. Because these remnants have such a high orbital periods and because the density of material in the solar nebula accretion disk decreases beyond Neptune, this material was unable to accrete into a planetary body. It has been postulated that the Kuiper Belt is responsible for supplying the low-inclination Jupiter-class comets. [Ref. 3]

III. DEFENDING THE EARTH AGAINST IMPACTS FROM LARGE COMETS AND ASTEROIDS.

A. INTRODUCTION

There are numerous illustrations of asteroid and comet impacts on Earth: meteorite craters, astroblems, and certain circular geologic structures. Many hypotheses have been formulated to predict the consequences of a collision with a Near Earth Object (NEO) with the Earth. Damage could be localized to a small geographical area, result in regional political instabilities, or cause devastating climatic change, dwarfing the feared “nuclear winter” damage of a global thermonuclear war. Recent research into the effects of a collision have fairly well established the evidence for severe climate alterations. The best known and most extensively investigated impact occurred on the Yucatan Peninsula, at the boundary of the Carboniferous and Paleogeneous Ages, 65 million years ago, and is thought to have caused the extinction of giant reptiles of that time. The geochemical and paleontological record has demonstrated that a 10- to 15-km diameter NEO impacted the Earth with the force of 100 million megatons in explosive energy. [Ref. 1] The frequency of such impacts is small but not insignificant.

The most energetic event of this century occurred over the Tunguska Valley in 1908. It was surmised that this event resulted from the break-up of a chondritic asteroid at an altitude of several kilometers. The explosive yield was originally estimated at 15–20 megatons (Mt) of TNT, although recent estimates have placed that number as high as 48 Mt, which leveled approximately 2,000 square kilometers of forest. [Ref. 9].

There are numerous ways of deflecting an Earth-crossing asteroid or comet. One involves a direct, kinetic energy type weapon, which imparts a change in momentum to the assailant object. A second way of mitigating the threat from an ECA or comet is through the use of nuclear explosive devices. Issues of great importance surrounding the

use of a nuclear device on a potential colliding object include: 1) estimating the radiation energy transfer to its surface; 2) maximizing radiation energy transfer; 3) understanding the hydrodynamic motion and mass blow-off from the surface, and the resultant momentum transfer; and 4) gaining knowledge of the various ways the object may be disrupted due to fracture or fragmentation. [Ref. 9]. Regardless of whether one of these, or some other method, is chosen, the several basic issues must be thoroughly understood before an attempt is undertaken to deflect an object.

The most likely candidate for mitigating the danger of an Earth impact is a rocket-delivered nuclear explosive. Nuclear explosive devices possess the highest concentration of energy, and can be manufactured with warheads yielding 100 Mt or more. A thermonuclear charge with a yield of 1 Mt has a mass of the order of 0.5 ton. Of interest is the fact that to obtain the equivalent energy by impact of a body of the same mass requires an impact velocity of approximately 4,000 km/s. [Ref. 9].

Simonenko et al. [Ref. 9] presents a list of problems that must be considered before the development of a defensive system could be undertaken.

1. Assessment of the number of dangerous cosmic bodies and their probability of their collision with the Earth.
2. Assessment of the time required to detect and identify them as dangerous.
3. Understanding of the object's motion in the immediate vicinity of the Earth, penetration of the atmosphere, and detailed dynamics during collision with the Earth, with concomitant assessment of the local and global consequences of the collision.
4. Assessment of the required effect on the astral assailant, whether it be deflection or fragmentation.
5. Consideration of the needed nuclear devices, delivery means, and optimal regime of action.
6. Assessment of consequences of collision with fragments of an object that had been fractured by a nuclear explosive.

7. Consideration of ecological consequences for the Earth and space environment of nuclear explosions in space.

The most important question from a technical viewpoint is to ascertain if it is feasible to significantly alter the trajectory of an ECA or comet by detonating a nuclear explosive near the surface. Equally as important is the ability to calculate the effects of such a weapon on the extraterrestrial body. Many characteristics of nuclear explosions are predictable and well defined. For example, detonation of a 100-kt device known as "Sedan" produces a crater 370 m in diameter and 100 m in depth. Significant differences may result by varying the nuclear explosion yield, distance to the target object, the object dimensions, material composition of the object, and the design of the nuclear device. Depending upon the interplay of these variables, the resultant explosion can result in fragmentation, crushing, or deviation of the target object from its initial trajectory. [Ref. 9].

Table 3 presents the yield vs. mass for nuclear explosive devices. This shows that the yield from current nuclear technology, that which can be launched with existing rocket technology, is capable of deflecting small objects. The nuclear device can be scaled upwards, perhaps an order of magnitude or more, while preserving special characteristics. In this case, modification would not require further testing. [Ref. 9] Of particular importance to the deflection of an asteroid are the specific physical characteristics of the body. These include shape, material composition, and physical stability of the object. Maximum effectiveness for deflection may require several nuclear devices detonated in a carefully determined sequence, or one device of special configuration. In addition, special measures can be taken to minimize the radiation contamination of the asteroid fragments, particularly important if it is determined that the fragments from such an explosion will continue towards impact with Earth.

Yield	Mass
1 Mt	0.5 ton
10 Mt	3 to 4 ton
100 Mt	20 to 25 ton

Table 3. Yield vs. Mass for Nuclear Devices [Ref. 9]

Finally, an area of study which needs additional study is that of the explosion of nuclear devices in space. Major differences include absence of atmosphere, commensurability of the object's dimensions with linear scales of the phenomenon, complexity of object shape, relatively weak gravity, and exotic material composition. [Ref. 9]

B. DEFLECTION CONSIDERATIONS

There are two main areas of interest in the mitigation of a Near-Earth Object (NEO): 1) causing the threatening object to break up, and 2) altering the trajectory of the object. There are several issues surrounding these areas which concern the scientific community with regard to deflecting or fragmenting a NEO sufficiently to avert collision with Earth. First, is there a limitation to the size of asteroid that can be deflected, given today's technology. Secondly, given the option, what is the most effective way to deflect these astral assailants to ensure, with a reasonable degree of certainty, that they will miss the Earth.

1. Size Limitations

Simonenko et al. [Ref. 9] has estimated the maximum dimensions of an object that can be influenced by a nuclear explosion as follows. Assume a nuclear explosion occurs on the surface of an asteroid having mass m_a and radius R_a . Assume the mass m of the material ejected by the explosion is small compared with the mass of the object. The mass of material ejected from the body has a distribution of velocities, but to simplify the estimation, it is assumed that all the ejected material has the same velocity,

the average of all the actual velocities, \bar{v}_m . This varies depending upon the explosive yield and material properties of the object.

Assuming $m \ll m_a$, conservation of momentum shows

$$m\bar{v}_\infty = m_a \Delta v_a \quad (3)$$

where \bar{v}_∞ is the velocity of the ejected material an infinity and Δv_a is the velocity increase of the object as a result of the explosion. In similar fashion, conservation of energy shows

$$-G \frac{m m_a}{R_a} + \frac{m \bar{v}_m^2}{2} = \frac{m \bar{v}_\infty^2}{2} + \frac{m_a (\Delta v_a)^2}{2} \quad (4)$$

where G is the universal gravitational constant. Combining Eqns. (3) and (4) gives

$$\bar{v}_\infty = \bar{v}_m \sqrt{1 - \frac{2Gm_a}{\bar{v}_m^2 R_a}}. \quad (5)$$

Examination of Eqn. (5) shows that if an asteroid is of sufficient mass, and given the above limitations on ejected material velocity, ejected material will simply fall back to the asteroid or remain in orbit around it, resulting in the object resuming its original velocity. To approximate the maximum radius and mass that could be deflected, Eqn. (5) solves for R_{acrit} with $\bar{v}_\infty = 0$. At this radius, all attempts to deflect the object are impossible by this method of explosion. The critical radius is defined as

$$R_{acrit} = \bar{v}_m \sqrt{\frac{3}{8\pi \rho_a G}} \quad (6)$$

where ρ_a is the average density of the object and

$$m_a = \frac{4}{3} \pi R_a^3 \rho_a. \quad (7)$$

Finally, the critical mass is given by

$$m_{acrit} = \frac{\bar{v}_m^3}{2G} \sqrt{\frac{3}{8\pi \rho_a G}}. \quad (8)$$

Knowles and Brode have published data showing that a conservative estimate of the ejection velocity, using currently available technology, is approximately 100 m/s. Using an average density of 5 g cm^{-3} for the assailant object, an average ejection velocity of 100 m s^{-1} for current technology, the critical mass and radius for the object are approximately $5 \times 10^{18} \text{ kg}$ and 60 km, respectively. Asteroids with masses or radii greater than these values cannot be deflected with current technology, regardless of the warning time involved. [Ref. 9]

2. Directional Considerations

The orbit perturbation requirements to deflect objects from collision with the Earth are an important consideration when planning a deflection mission. Two scenarios are considered: (1) A short time-scale deflection where equations of motion are linearized, and (2) A long time-scale deflection, using orbital equations of motion. These two scenarios are developed fully below, the results of which will be used to generate the change in velocity requirements for a hypothetical asteroid.

a. *Short Time-Scale Deflection*

The short time-scale deflection scenario is easily developed using rectilinear equations of motion. This is valid if the time scale involved is short compared to the orbital period, P . To prevent a collision, a change in velocity must be imparted orthogonal to the flight path of the object. The displacement, δ , that must be achieved by a change in velocity, Δv , is

$$\delta = \Delta v \cdot t. \quad (9)$$

Assuming the object were on a path such as to intersect the center of mass of the Earth, the object must be deflected a minimum of one Earth radius. This provides no margin of safety, however, and therefore, taking the minimum acceptable distance to

be two Earth radii, the minimum change in velocity required to deflect a potential threat is given by

$$\Delta v \approx \frac{2R_{\oplus}}{t} \approx \frac{147.6 \text{ ms}^{-1}}{t, \text{ days}}. \quad (10)$$

b. Long Time-Scale Deflection

For a deflection to be accomplished over a longer period of time, the equations of motion cannot be simplified to the rectilinear case and the two-body orbital mechanics equations of motion apply. There are three directions with respect to the flight path which will cause an orbiting body to deviate from the original orbit: (1) orthogonal to the flight path, along the line parallel to the angular momentum vector, (2) orthogonal to the flight path, in the plane of the orbit, and (3) along the flight path, in the orbit plane. A two body circular orbit is assumed to simplify the problem.

Given a longer response time, the best deflection direction may not be orthogonal to the flight path direction, as in the short time-scale deflection. Each option is assessed below to determine the optimal deflection direction.

(1) Out of plane, orthogonal to flight path. A change in velocity made orthogonal to the orbit plane, as shown in Figure 10, results in a change of inclination according to

$$\Delta v = 2v \sin \frac{i}{2}, \quad (11)$$

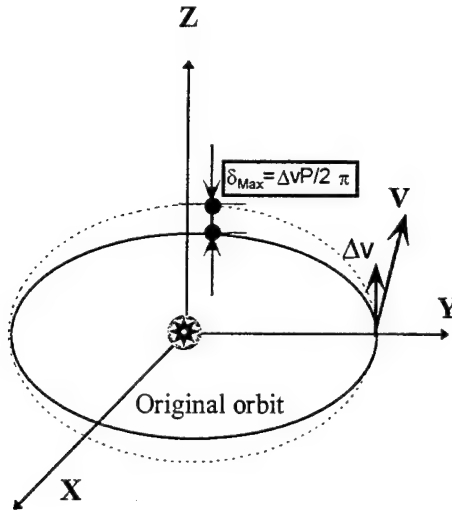


Figure 10. Deflection Out of Plane, Orthogonal to Flight Path.

where v is the orbital speed of the object and i is the required inclination change. The maximum displacements occur $\pi/2$ and $3\pi/2$ around the orbit. The orbital period remains unchanged. Using a small angle approximation gives

$$\Delta v \cong vi \cong v \frac{\delta}{r} \quad (12)$$

where δ is the amount the body's orbit will be deflected $\pi/2$ past the point of the deflection, and r is the radius of the object's orbit around the Sun. Finally, substituting in for the orbital velocity in terms of orbital period, P , gives

$$\Delta v \cong 2\pi \frac{\delta}{P}. \quad (13)$$

Conversely, the maximum distance the orbit may be changed is found using

$$\delta_{\max} \cong \Delta v \frac{P}{2\pi}. \quad (14)$$

The minimum change in velocity required to deflect the asteroid two Earth radii is given by

$$\Delta v \cong \frac{4R_e\pi}{P}. \quad (15)$$

For a circular orbit at 1 AU, the minimum change in velocity required to achieve the required deflection is approximately 2.54 m/s and should be imparted 90° prior to the expected impact point in the asteroid's orbit.

(2) In plane, orthogonal to flight path. The change in velocity required to deflect an object using a deflection in the asteroid's orbital plane, orthogonal to the flight path is found in a manner similar to (1), above. As before, the orbital period remains the same. The asteroid is displaced along it's track with the maximum displacement occurring $\pi/2$ and $3\pi/2$ around the orbit, as shown in Figure 11. The maximum deflection

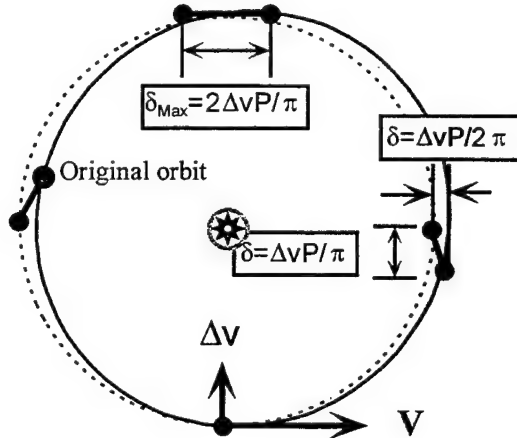


Figure 11. Deflection In Plane, Orthogonal to Flight Path.

is

$$\delta_{\max} \cong \frac{2\Delta v P}{\pi} \quad (16)$$

and the minimum change in velocity required to deflect the asteroid two Earth radii is given by

$$\Delta v \cong \frac{R_e \pi}{P}. \quad (17)$$

The required change in velocity for this case is approximately 0.635 m s^{-1} .

(3) In plane, along flight path. A deflection along the flight path, shown in

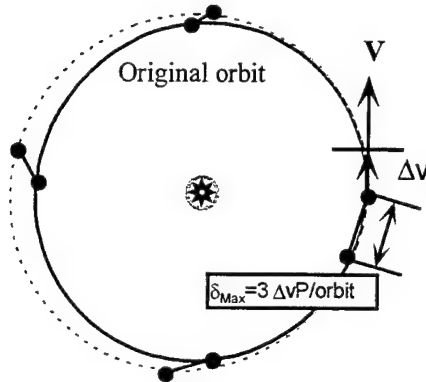


Figure 12. Deflection Along Flight Path.

will result in a net increase or decrease in the orbital speed. If there is a net increase in speed, the point at which the deflection occurred will be the perihelion of a new orbit. Conversely, if there is a net decrease in speed, the deflection point will be the aphelion of a new orbit. Irrespective of deflection direction, the period of the deflected object's orbit will change. This change in period serves as the mechanism by which, over time, an object can be influenced so as to miss a collision with the Earth. The amount the asteroid is displaced during each orbit is directly proportional to the change in period effected by the deflection. This is given by

$$\delta_{\text{per-orbit}} = v \Delta t. \quad (18)$$

The approximate displacement for a deflection along the flight path can be derived from the equations for the specific mechanical energy of a body,

$$E = \frac{v^2}{2} - \frac{\mu}{r} = \frac{-\mu}{2a}, \quad (19)$$

the orbital period of a body,

$$T = 2\pi \sqrt{\frac{a^3}{\mu}}, \quad (20)$$

and the circular velocity for an orbit,

$$v = \sqrt{\frac{\mu}{a}}. \quad (21)$$

Taking the derivative of Eqn (19) and substituting v^2 for μ/a gives

$$\frac{\Delta v}{v} = \frac{\Delta a}{2a}, \quad (22)$$

while taking the derivative of Eqn. (20) and resubstituting in for T gives

$$\Delta T = 3T \frac{\Delta a}{2a}. \quad (23)$$

Substituting (22) and (23) into (18) gives the maximum deflection per orbit, in terms of the original orbital period of the asteroid and the change in velocity imparted to the object, as

$$\delta_{per-orbit} = 3T\Delta v. \quad (24)$$

So, the change in velocity required to deflect an object two Earth radii is approximately

$$\Delta v = \frac{2R_e}{3nT} \quad (25)$$

where n is the number of orbits prior to impact. If n = 1, the change in velocity is approximately 0.135 m s^{-1} . This is better than either case (1) or (2). If the impact can be predicted as much as a decade in advance, the change in velocity required to deflect the asteroid is reduced to 1.35 cm s^{-1} . This is an order of magnitude less than case (2) and two orders of magnitude less than case (1) and is an achievable quantity in terms of technological feasibility.

IV. DEVELOPMENT OF HYPOTHETICAL ORBITS

A. INTRODUCTION

In order to accurately test the sensitivity of the change in velocity requirements presented in section III, accurate orbital parameters for hypothetical asteroid objects were first developed. This section first describes the coordinate systems used and the characteristics of circular, elliptical, parabolic, and hyperbolic orbits. Next, this section describes the process by which the Earth's position in heliocentric coordinates, at any given time, are used to generate the heliocentric coordinates of an intersecting asteroid orbit. The size, shape, and inclination of the asteroid orbit are variables defined by the user with the only limitation being that the two orbits intersect. MATLAB scripts which generate these procedures are contained in the Appendix. Orbits can be generated for circular, elliptical, parabolic, or hyperbolic trajectories.

Development of hypothetical orbits followed a rigorous routine allowing for repeatability of the work done while minimizing the workload for completing multiple simulations. The methodology and theory used in the development of the MATLAB scripts are discussed below.

B. COORDINATE SYSTEMS

The first requirement for describing an orbit is to define a suitable reference frame. In many cases this means finding an appropriate inertial coordinate system. For orbits around the Sun such as planets, asteroids, and comets, the heliocentric-ecliptic coordinate system is often used. Satellites in orbit around the Earth use the geocentric-equatorial system. [Ref. 10] Another convenient coordinate frame used for describing the orbit of a body is the perifocal coordinate system. Each rectangular coordinate frame is defined by specifying the origin, the fundamental plane (i.e. the X-Y plane), and the direction of each axis. In developing the hypothetical orbits used for the simulations, the

heliocentric-ecliptic and perifocal coordinate systems were used extensively. These are described in detail below.

1. Heliocentric Ecliptic Coordinate System

The heliocentric-ecliptic coordinate system, as the name implies, has its origin at the center of the Sun. The letters XYZ describe the three principle axes as shown in Figure 13. The fundamental plane, the X-Y plane, coincides with the ecliptic, which is the

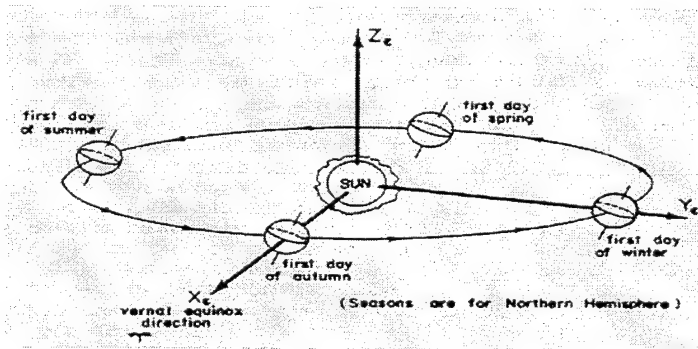


Figure 13. The Heliocentric-Ecliptic Coordinate System. From Ref. 10.

plane defined by the Earth's orbit around the Sun. The line of intersection of the Earth's equatorial plane and the ecliptic plane (XY) where the Sun crosses the equator from south to north in its apparent annual motion along the ecliptic is known as the vernal equinox. When the vector from the Earth to the Sun (X-axis) points towards what is now approximately the constellation of Pisces, it coincides with the vernal equinox, also known as the first day of spring. The Y axis is 90° from the Z axis in the direction of the Earth's rotation around the Sun. The Z axis completes the right-handed coordinate system. [Ref. 10]

2. Perifocal Coordinate System

The perifocal coordinate system, shown in, Figure 14, is one of the most useful coordinate systems for describing the motion of a body. The letters PQW are used to

describe the three principle axes. The fundamental plane, the PQ plane, is in the plane of the body's orbit and the origin is at the focus of the primary body, in our case the Sun. The P axis is in the direction of perihelion while the Q axis is 90° from the P axis in the direction of rotation. The W axis completes the right-handed coordinate system.

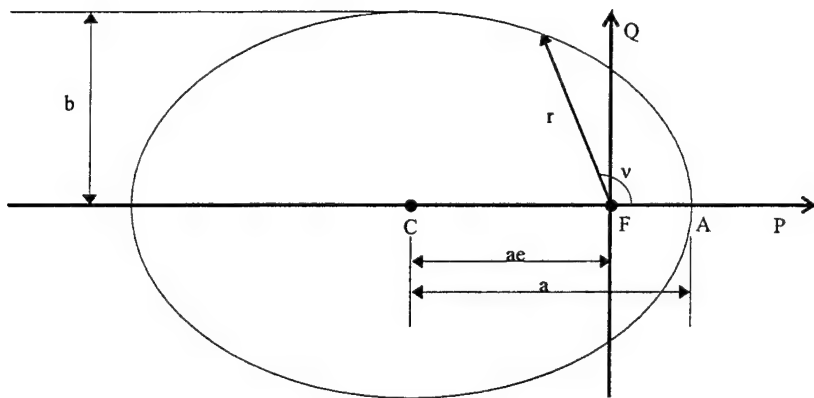


Figure 14. Perifocal Coordinate System.

C. CLASSICAL ORBITAL ELEMENTS

Five classical orbital elements, also known as Keplerian elements, are sufficient to describe the size, shape, and orientation of an orbit. A sixth element is required to locate a body in that orbit.

There are many ways of locating the position of a body in the orbit plane which may be substituted for time of perihelion passage.

1. True anomaly at epoch, v_o , is the angle in the plane of the body's motion measured from perihelion to the position to the body at a given time (epoch).
2. Argument of latitude at epoch, u_o , is the angle in the plane of the orbit between the longitude of the ascending node and the radius vector to the body at a given time. If ω and v_o are both defined then

$$u_o = \omega + v_o. \quad (26)$$

If there is no ascending node, as in an equatorial orbit, then both ω and u_0 are undefined.

3. True longitude at epoch, l_0 , is the angle measured between \mathbf{X} and \mathbf{r} , the radius vector to the body, measured eastward to the ascending node, if it exists, and then in the orbital plane to \mathbf{r} . If Ω , ω , and v_0 are all defined, then

$$l_0 = \Omega + \omega + v_0 = \Pi + v_0 = \Omega + u_0. \quad (27)$$

Two other terms used in the descriptions of orbits are direct, or prograde, and retrograde. Direct means easterly, in accordance with the right-hand rule, and is the same direction in which the Sun, Earth, and most of the planets and their moons rotate on their axes and the direction in which all planets rotate around the Sun. A retrograde orbit, as the term implies, is the opposite of direct. Table 4 provides a summary of the various types of orbits and the orbital parameters that result.

Parameter	Circle	Ellipse	Parabola	Hyperbola
Eccentricity	$e=0$	$0 < e < 1$	$e=1$	$e > 1$
Energy	$-\mu/2a < 0$	$-\mu/2a < 0$	$E=0$	$\mu/2a > 0$
Period	$P=2\pi/n$	$P=2\pi/n$	-	-
Anomaly	Undefined or arbitrary	Eccentric: $\tan \frac{v}{2} = \frac{(1+e)^2}{(1-e)} \tan \frac{E}{2}$	Parabolic, D: $\tan \frac{v}{2} = \frac{D}{\sqrt{2q}}$	Hyperbolic, F: $\tan \frac{v}{2} = \frac{(1+e)^2}{(1-e)} \tanh \frac{F}{2}$

Table 4. Keplerian Orbits

D. DERIVATION OF FORMULAE

1. Procedure

a. *Orbital Elements From r and v*

Conversion from position and velocity vectors to orbital elements is done using standard procedures. For the purposes of this example, the Earth's orbital parameters are being determined from position and velocity vectors.

First the angular momentum is determined. From the relative form of the basic two-body equation

$$\ddot{\vec{r}} = -\frac{\mu}{r^3} \vec{r}. \quad (28)$$

Cross multiplying both sides by the position vector, \vec{r} , gives

$$\vec{r} \times \ddot{\vec{r}} + \vec{r} \times \frac{\mu}{r^3} \vec{r}. \quad (29)$$

Expanding this equation, one then finds the angular momentum

$$\vec{h} = \vec{r} \times \vec{v} = \text{constant}. \quad (30)$$

The vector pointing to the node is then calculated using

$$\vec{n} = \vec{K} \times \vec{h} \quad (31)$$

where K is the unit vector in the Z direction. If the magnitude of the node vector is zero, the orbit is in the fundamental plane. The MATLAB script used to calculate this vector has a filter to set the vector equal to zero if the magnitude is less than 1×10^{-5} .

Next the eccentricity vector is calculated with

$$\vec{e} = \frac{1}{\mu} \left[\left(v^2 - \frac{\mu}{r} \right) \vec{r} - (\vec{r} \cdot \vec{v}) \vec{v} \right]. \quad (32)$$

The magnitude of this vector provides the eccentricity. It is important to realize that this vector is zero for circular orbits.

The semi-latus rectum, p , is calculated

$$p = \frac{h^2}{\mu} \quad (33)$$

as are the semi-major axis

$$a = \frac{p}{1 - e^2} \quad (34)$$

and the radius at aphelion and perihelion

$$r_a = \frac{p}{1-e}, r_p = \frac{p}{1+e}. \quad (35)$$

Once the size and shape parameters have been determined, all that remains is to find the orientation of the Earth's orbital plane and the position of the Earth in that orbit. First, the inclination is found with

$$\cos(i) = \frac{\vec{h} \cdot \hat{K}}{|\vec{h}|}. \quad (36)$$

There is no need to check for angle ambiguities as the inverse cosine always returns an angle between 0° and 180° .

Next, the longitude of the ascending node, which varies from 0° to 360° must be determined. By definition, the Earth is in the mean ecliptic and the inclination is zero deg. By convention, the longitude of ascending node is defined to be zero deg; there is no real "ascending node". However, due to small perturbations in the Earth's orbit around the Sun, the center of mass of the Earth deviates out of the mean ecliptic to what is known as the true ecliptic. As a result, when there are instantaneous components of the position and velocity vector normal to the mean ecliptic, very small, but calculable values for inclination can be found. Also, a value for the longitude of ascending node can be found. If the instantaneous position and velocity vectors lie in the plane of the ecliptic, the longitude of ascending node and inclination are zero deg. and the only rotation is that of the argument of perihelion. As mentioned previously, orbits aligned with the fundamental plane, in our case the ecliptic, have no node vector and the longitude of the ascending node is undefined. However, a value for the majority of orbits is obtained from

$$\cos(\Omega) = \frac{\hat{I} \cdot \vec{n}}{|\hat{I}| |\vec{n}|}. \quad (37)$$

In this case a quadrant check must be conducted and if the dot product of \mathbf{J} and \mathbf{n} is less than zero, then Ω must lie between 180° and 360° .

The argument of perihelion, which also varies from 0° to 360° is calculated. Again, this value is undefined for circular orbits and orbits in the ecliptic because perihelion does not exist for the former and there is no node vector in the later.

$$\cos(\omega) = \frac{\vec{n} \cdot \vec{e}}{|\vec{n}||\vec{e}|}. \quad (38)$$

Angle ambiguities are resolved by computing the dot product of \mathbf{K} and \mathbf{e} . If this value is less than zero, then perihelion is below the ecliptic and the argument of perihelion is between 180° and 360° .

The final classical orbital element is the true anomaly at epoch, which can vary from 0° to 360° . As mentioned previously, the true anomaly is the angle in the orbit plane measured from perihelion to the Earth's current position. The true anomaly is then

$$\cos(v) = \frac{\vec{e} \cdot \vec{r}}{|\vec{e}||\vec{r}|}. \quad (39)$$

The correct quadrant for the true anomaly is found from the dot products of \mathbf{r} and \mathbf{v} . If the dot product is less than zero, then the true anomaly is between 180° and 360° .

b. *Singularity Solutions*

Several special cases must be considered, especially when calculating values for the orbital elements using a computer routine. The first occurs when the orbital plane is the same as the fundamental plane. This is especially relevant to the orbit of the Earth around the Sun. By definition, the Earth is in the ecliptic, the inclination and longitude of ascending node are zero and the normal equation to calculate the argument of perihelion cannot be used. However, the instantaneous position and velocity vectors may contain small components out of the plane of the mean ecliptic. There are small values for inclination and longitude of the ascending node. To obtain the required accuracy, these angles are included when calculating the asteroid's orbit. Appropriate

filters handle the case when the Earth's position lies exactly in the mean ecliptic, and the inclination and longitude of ascending node are zero.

These singularities are removed by using the true longitude of perihelion, ϖ_{true} , which combines Ω and ω . It is found through

$$\cos(\tilde{\omega}_{\text{true}}) = \frac{\hat{J} \cdot \bar{e}}{|\hat{J}||\bar{e}|} \quad (40)$$

which is valid for elliptical orbits which lie in the ecliptic. Again, a quadrant check is necessary and is found using the dot product of \mathbf{J} and \mathbf{e} . If this value is less than zero, the true longitude of perihelion is between 180° and 360° .

c. Orbital Anomaly Determination

There are several other useful formulas that must be derived prior to writing script files for the plotting of orbits and calculation of orbital parameters. First, for elliptical orbits, such as those of the Earth, ECAs, and short-period comets, formulas for determining the eccentric anomaly and the true anomaly prove quite useful. Figure 15 shows an x,y Cartesian coordinate system centered at C . F is the focus of an ellipse, in this case the Sun. An auxiliary circle of radius a with center C is constructed. P is the location of the Earth in its orbit about the Sun and Q is the point where the perpendicular to the semi-major axis intersects the auxiliary circle. The angle E is the eccentric anomaly and ν is the true anomaly of the point P .

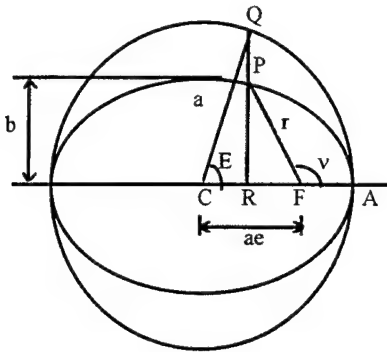


Figure 15. Orbital Anomalies for Elliptic Motion

The x and y coordinates of the ellipse can be expressed in parametric form as

$$x = a \cos E \quad y = b \sin E. \quad (41)$$

for the coordinate system centered at C, shown above. If the focus is selected as the center of the coordinate system, the radial position of the point P can be expressed in terms of E using the general form of for the radial position of an ellipse with the origin at the center

$$r = a - ex \quad (42)$$

so that

$$r = a(1 - e \cos E). \quad (43)$$

Comparing this to the polar equation of the ellipse

$$r = \frac{a(1 - e^2)}{1 + e \cos v} \quad (44)$$

the identities for true anomaly and eccentric anomaly are obtained as

$$\cos v = \frac{\cos E - e}{1 - e \cos E} \quad \cos E = \frac{e + \cos v}{1 + e \cos v}. \quad (45)$$

The true anomaly for the body is obtained by solving Eqn. (44).

$$v = \arccos \left(\frac{1}{e} \left(\frac{p}{r} - 1 \right) \right) \quad (46)$$

Another identity, Gauss' law, provides a useful relation between v and E.

$$\tan \frac{1}{2}v = \sqrt{\frac{1+e}{1-e}} \tan \frac{1}{2}E. \quad (47)$$

Because $1/2 v$ and $1/2 E$ are always in the same quadrant, there is no angle ambiguity to resolve when solving this form of the equation.

2. Determination of r and v From Intersecting Orbit Parameters

From a given orbit and the position of a body within that orbit, a second orbit can be constructed which intersects the first orbit. The location of a body within the second orbit which intersects the body in the first orbit is specified by the formulation of the solution. Values for semi-major axis, eccentricity, and inclination are variables and can be any value with the only limitation that the two orbits must have at least one point of intersection. Finally, the position and velocity vectors in the new orbit at the point of intersection are calculated. These position and velocity vectors are in perifocal coordinates. The detailed procedure for calculating these vectors is presented below.

a. Circular, Elliptical, and Hyperbolic Orbits.

The polar equation for an ellipse

$$r = \frac{a(1-e^2)}{1+e \cos v} \quad (48)$$

can be used to solve for the true anomaly at epoch. The magnitude of r in this equation is the magnitude of the Earth's position vector at epoch. Once the true anomaly at epoch is known, the position vector in the perifocal coordinate system can be determined using

$$\vec{r} = r \cos v \hat{P} + r \sin v \hat{Q} \quad (49)$$

where the magnitude of r is once again the magnitude of the Earth's position vector and epoch.

Differentiating Eqn. (49) in this "inertial" perifocal frame gives

$$\vec{v} = \dot{\vec{r}} = (\dot{r} \cos v - r \dot{v} \sin v) \hat{P} + (\dot{r} \sin v + r \dot{v} \cos v) \hat{Q}. \quad (50)$$

Substituting in

$$\dot{r} = \sqrt{\frac{\mu}{p}} e \sin v \quad r\dot{v} = \sqrt{\frac{\mu}{p}} (1 + e \cos v) \quad (51)$$

gives

$$\bar{v} = \sqrt{\frac{\mu}{p}} [-\sin v \hat{P} + (e + \cos v) \hat{Q}] \quad (52)$$

b. *Parabolic Trajectories.*

The semi-major axis of a parabolic orbit is undefined. If the desired orbit is parabolic in shape, the parameter, p , is substituted for the semi-major axis. The polar equation of the parabola is then

$$r = \frac{p}{1 + \cos v}. \quad (53)$$

This equation is solved for v , as discussed previously. The formulas for calculating the position and velocity vectors in perifocal coordinates are then identical to the elliptical case discussed previously.

3. Orbit Rotations

Rotations between coordinate frames are accomplished using Direction Cosine Matrices (DCMs). Coordinate rotations may be accomplished by any number of methods. One common method of conducting coordinate rotations is through a 3-1-3 rotation: A rotation about the 3-axis, followed by a rotation about the new 1-axis, and finally a 3-rotation about the new 3-axis. An example, shown in Figure 16, converts from perifocal coordinates to Heliocentric-ecliptic coordinates. The rotation matrices as a function of angle of rotation, α , are presented below. The subscript associated with each transformation is the axis about which the rotation is to be accomplished.

$$C_1(\alpha) = \begin{bmatrix} 1 & 0 & 0 \\ 0 & \cos\alpha & \sin\alpha \\ 0 & -\sin\alpha & \cos\alpha \end{bmatrix}. \quad (54)$$

$$C_3(\alpha) = \begin{bmatrix} \cos\alpha & \sin\alpha & 0 \\ -\sin\alpha & \cos\alpha & 0 \\ 0 & 0 & 1 \end{bmatrix}. \quad (55)$$

Transforming an orbit expressed in perifocal coordinates to heliocentric coordinates is conducted through the following formulations:

$$\vec{r}_{JK} = C_3(\omega)C_1(i)C_3(\Omega)\vec{r}_{PQW}. \quad (56)$$

$$\vec{v}_{JK} = C_3(\omega)C_1(i)C_3(\Omega)\vec{v}_{PQW}. \quad (57)$$

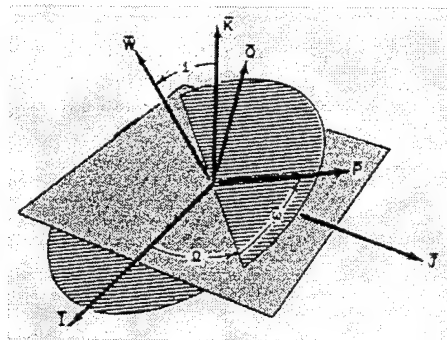


Figure 16. Coordinate Transformations. From Ref. 10.

V. CASE STUDIES.

A. INTRODUCTION

Two tests were conducted to analyze the effects of orbital perturbations on an assailant asteroid. The magnitude of the velocity applied, is the change required along the flight path, to change the orbital period of a circular orbit such that the change in position after one orbit is equal to two Earth radii. This magnitude is approximately 13.5 cm/sec/orbit. The first used a solar system simulation modeling program called *Dance of the Planets*. [Ref. 4] This program, described in further detail below, allows the user to input hypothetical objects into a relatively high fidelity simulation of the solar system. It includes gravitational models for the Sun and all of the planets. Objects can be imported into the program using their orbital elements or their position and velocity vectors at a given time. The model then calculates new orbital positions and velocities for each body included in the model using a full gravitational model. The simulation accurately computes both forward and backward in time. Although the program provides a reasonable model visualization, an inaccuracy was discovered during testing which prevented importing of position and velocity vectors of sufficient accuracy for valid tests to be conducted. This inaccuracy is demonstrated and explained in section 7 of this chapter. The discussion focuses on the procedure used to generate the desired asteroid vectors. This would prove useful for follow-on research should the program be modified to provide the required accuracy.

The second method used to evaluate sensitivity of deflection distance and direction to variations in orbit eccentricity and size (semi-major axis) consisted of a relatively simple model to determine miss distance based on the asteroid's mean anomaly, M , and mean motion, n . The position and velocity vectors at some time prior to collision were calculated, new orbital elements determined, and the new position at the original

time found. The distance between the center of the Earth's orbit and the asteroid's orbit was then calculated. The effect of varying specific orbital parameters while keeping the magnitude of the change in velocity constant were analyzed. Parameters varied were orbital eccentricity, semi-major axis, and deflection direction.

B. DANCE OF THE PLANETS

1. Hypothetical Orbit Determination

The purpose of this section is to present the process used to calculate asteroid object orbital elements and heliocentric coordinates from the Earth's heliocentric coordinates. The position and velocity vectors obtained are the position of the asteroid in its new orbit around the sun in heliocentric coordinates. This is exactly the same position as that of the Earth, hence collision. The asteroid's velocity vector is that vector which meets the size and shape requirements dictated earlier in the orbit development process and is the asteroid's instantaneous velocity vector at collision. These vectors are then imported into *Dance of the Planets* at the epoch for which the Earth's original \mathbf{r} and \mathbf{v} were obtained. The orbit was then propagated backwards in time. New velocity vectors with a delta-v applied were calculated and imported into the program. These new vectors were propagated forward to determine if collision had been averted. The procedure, summarized here, is described in detail in the sections which follow.

- a. First, the Earth's orbital elements are calculated from \mathbf{r} and \mathbf{v} .

Specifically, true anomaly, ν , is required so that the position in the orbit is known.

- b. The asteroid's orbit size, shape, and inclination (a , e , and i) are selected.
 - c. The asteroid's orbital elements are calculated in perifocal coordinates.
 - d. The asteroid's orbit in perifocal coordinates is rotated, using a 3-1-3 rotation, to make it coplanar with the Earth's orbit. The eccentricity

vectors are aligned. This makes the Sun and the two orbit's perihelions collinear.

- e. A second 3-1-3 rotation is performed to obtain the desired inclination and align the two \mathbf{r} vectors. The first 3-rotation is through an angle v_{earth} and aligns the asteroid's perihelion with the position of the Earth in its orbit. The 1-rotation inclines the orbit to the desired value. The final 3-rotation, through an angle $-v_{\text{asteroid}}$, aligns the asteroid with the Earth's current position.

2. Initialization.

The first step in the development of hypothetical orbits and completing the simulation of Near Earth Objects (NEOs) was to select a desired date and time for the impact. For the purposes of this research, the date chosen was January 01, 2007 at 00:00 UT. This date was selected as it gave a real world flavor to the problem, approximately one decade would elapse from the time of discovery to the time of impact. Universal Time (UT) is the standard time in the time zone centered on zero degrees longitude in Greenwich, England. UT is used for calculating where an object is in the sky relative to the horizon at a particular location.

Next the position and velocity vectors for Earth at the desired impact date were obtained from *Dance of the Planets*. The operator's manual contains an excellent tutorial and provides the information required to operate the program. Several preliminary steps must be completed prior to date initialization. The simulation is initialized from Space View. Second, from the main access screen, any planets that are to be excluded from the gravitational model are deselected. This is indicated by a zero in the on column next to the planet name. Returning to the simulation Space View, confirm the simulation pace is set to true time. This minimizes the elapsed time upon returning to the simulation after

initializing the date. In addition, this also minimizes the change in planetary position and velocity vectors during the time from initialization to reselecting the main access facilities display where the Earth's vectors are obtained. Finally, enter the desired date. Digital hours and minutes appear at low simulation paces. Local time, determined by site longitude, is shown unless time is offset.

Immediately after entering the desired date, reenter the main access screen. For each planet selected, *Dance of the Planets* calculates the period, the distance to the Earth and Sun in astronomical units (AU), heliocentric longitude (calculated and simulated), right ascension of the ascending node, declination, and apparent magnitude. The difference between calculated and simulated heliocentric longitude is that the calculated value is the position as determined from ephemeris equations while the simulated value gives the position in "simulator space." Comparison of the two values provides an accuracy check for the user between the ephemeris equations and the *Dance of the Planets* model.

The instantaneous position and velocity vectors of the planets provide the essential information to describe dynamic state. With these datum the six orbital parameters of eccentricity, semi-major axis, right-ascension of the ascending node, inclination, argument of perihelion, and true anomaly, can be calculated.

3. Constants

The program provides the user with the option of obtaining the position and velocity vectors or the orbital elements at a given epoch. The display shows the calculated vectors for the planets in heliocentric coordinates, XYZ, as well as the epoch Julian date. Units for the position and velocity vectors are E6 km and km/sec, respectively. The epoch date is presented in the form 24dddddd.ffff and is reference to the epoch (equinox) of the year 2000 (J2000), as are contemporary star charts. Only Julian dates beginning with 24dddddd can be used, giving a 14,680 year window for simulations.

[Ref. 4] Mean planetary constants for epoch J2000 of the Earth are given in Table 5.

Solar constants are shown in Table 6.

Parameter	Value
Semi-major axis	
AU	1.000 001 017 8
km	149,598,023
Eccentricity	0.016 708 617
Inclination ~ deg.	0.000 000 000
Long. of ascending node (Ω) ~ deg	0.000 000 00
Long. of perihelion (ω) ~ deg	102.937 348 08
True longitude (L) ~ deg	100.466 448 51
Orbital period (P) ~ years	0.999 978 62
Orbital velocity (v) ~ km/s	29.77859
Equatorial radius (R_e) ~ km	6378.137
Gravitational parameter (μ) ~ km ³ /s ²	3.986x10 ⁵
Mass (M_e) ~ kg	5.9742x10 ²⁴
Rotation ~ days	0.997 269 69
Inc. of equator to ecliptic ~ deg	23.45
Density ~ gm/cm ³	5.515

Table 5. Mean Earth Constants for Epoch J2000

Parameter	Value
Radius of the Sun (R_s) ~ km	696,000.000
1.0 AU ~ km	149,597,870.0
1.0 AU/TU _{sun} ~ km/solar s	29.784 691 674 9
Gravitational parameter (μ) ~ km ³ /s ²	1.327 124 28x10 ¹¹
1.0 TU ~ solar days	58.132 440 9

Table 6. Solar Constants

4. Orbital Element Selection

The orbital elements selected for simulation, shown in Table 7, were selected from a list of all known ECA's given by Rabinowitz et. al. [Ref. 5] and [Ref. 7]. These were selected because they each have a point of close approach distance within 20 lunar

radii over the course of the next century, and because they are representative of each class of asteroid as well as a short-period comet.

No. and Name	H	Approx. diameter (km)	Depth (AU)	q (AU)	a^1 (AU)	e^1	i^1 (deg)
2340 Hathor	20.26	0.2	0.356	0.464	0.844	0.450	5.85
4660 Nereus	18.30	1	0.092	0.954	1.490	0.360	1.43
4179 Toutatis	14.0	5	—	0.542	2.505	0.640	0.47
Encke	9.8	—	—	0.331	2.283	0.855	11.9

Note: (1) Values used in the development of the hypothetical orbit

Table 7. Selected Near-Earth Objects Used for Simulation Study.

5. Asteroid Orbit Rotations

Two series of 3-1-3 rotations are used to achieve the desired orbit. The first series of rotations transforms the position and velocity vectors from perifocal coordinates to the Earth's orbital plane. These angles were previously calculated and are the Ω , i , ω rotation angles. Because the true ecliptic is used, the Earth's orbit with respect to the mean ecliptic is found using the three rotations calculated in Eqns. (37), (38), and (39), inclination, longitude of ascending node, and argument of perihelion, respectively.

Once the assailant object's orbit is coplanar with that of Earth, and the eccentricity vectors are aligned, a second 3-1-3 coordinate transformation is accomplished. This series of rotations serves two important purposes: (1) they rotate the orbit to the desired inclination, and (2) they align the position vectors of the Earth and the asteroid.

The first 3-rotation, through the angle ν_{earth} , aligns the object's eccentricity vector, which points towards perihelion, with the Earth's position vector. The 1-rotation, about the eccentricity vector, effects the desired value of inclination. The final 3-rotation about the orbit normal, though an angle $-\nu_{\text{asteroid}}$, aligns the asteroid's position vector with the Earth's position vector.

6. Simulation

Once the position and velocity vectors are calculated, they are inserted into *Dance of the Planets* as object vectors. The fictitious orbit, at epoch, is one having the same \mathbf{r} as Earth but with a velocity vector as provided by MATLAB to provide the desired orbit size and shape.

The simulation is run backwards in time to an arbitrary time. This will be the new start time of the simulation. At this point, the simulation is paused, and the new orbital elements are calculated for the asteroid's current orbital set. These are not the same as the original orbit's parameters due to the influence of third bodies on the asteroid's orbit during the simulation period. Specifically, the influence of the Earth on the asteroid's orbit during the first month of the reverse simulation has a significant impact on the orbital parameters.

Next, another MATLAB script file uses the current orbital parameters to recalculate the velocity vector of the assailant body for a desired delta-V applied to the body at a given time. This procedure is described in detail below.

Finally, the simulation was run forward in time to determine if *Dance of the Planets* achieved the simulation accuracy required to show the deflection of the asteroid and determine if the calculated deflection is sufficient to avoid collision. The results are presented in the next section.

All MATLAB scripts, presented in the Appendix, were written in modular fashion. Running the script from the main program accesses additional script files as required. Each file can also be run from the Command window by typing the function name with the appropriate arguments provided. Help files are provided for each function file. The MATLAB scripts also plot the Earth and asteroid orbits. Aphelion, perihelion, the position of each body in their orbits is indicated on the plots.

7. Results and Discussion.

Following the development of the MATLAB function files and orbital development routines, a problem was discovered with the accuracy of files imported to *Dance of the Planets*. Data files used to import elements into the simulation are space delimited and of the form :

Name	x	y	z	Vx	Vy	Vz	epoch
------	---	---	---	----	----	----	-------

The position coordinates were in units of E6 km and contained up to 5 decimal place precision. Velocity vector components were in km/sec and contained up to 6 decimal place precision. Epoch date was in Julian days and allowed inputs up to four decimal places.

Importing a data file with this level of exactness would have been sufficient to accurately test the deflection hypothesis presented in section III. However, when data was imported, the values obtained were slightly different from the original file. Table 8 show the result of importing the data file for asteroid 2340 Hathor. The file contained the consisted of the position and velocity vectors shown under Hathor, below, and was obtained by exporting actual position and velocity data from *Dance of the Planets*. The example column listed next to Hathor shows how the values differed following importation.

Ast.	Hathor	Example
x	13.29207	13.29217
y	-75.41408	-75.41404
z	0.02352	0.02351
Vx	44.735765	44.735756
Vy	19.744673	19.744721
Vz	-4.868622	-4.868622

Table 8. Imported Asteroid's Altered Position and Velocity Vectors.

The magnitude of the change between the desired values and the values as altered by *Dance of the Planets* is shown in Table 9. If the values had been imported correctly the position and velocity vectors would be identical.

Asteroid	Delta r (km)	Delta v (m/s)
Example	108.1665	0.1082

Table 9. Position and Velocity Change from Original Orbit.

While these errors were relatively small, they were of sufficient magnitude to impart significant errors at the initiation of the simulation and prevented precise and accurate testing of the theories; the magnitude of the change in velocity to be imparted to the asteroid was of approximately the same magnitude as the error generated by the program. Additionally, these errors were not consistent in magnitude or direction from one test to the next. The errors could not be biased out by altering the date of epoch for the simulation.

Discussions with Terry Hannon of Applied Research & Consulting, Inc., one of the software developers for the program, lead to speculation that the problem may lie in the precision of the epoch currency. The program presents accuracies to one ten-

thousandth of a day, approximately eight seconds, while the accuracies required for the thesis testing was on the order of one second accuracy. In fact, although the epoch date is displayed out to four decimal place, the manufacturer believed the program accuracy to be somewhat less than this.

The program is written in Pascal, and should the manufacturer make it available, the code could perhaps be modified so as to make it acceptable to conduct simulations of this type. Several simulations were conducted which did not require the importation of data files. These runs were very accurate and results were repeatable during multiple simulations. Overall, the program provides very accurate orbital positional data for predicting and visualizing solar system events. Without modification, however, the program is not sufficiently precise to conduct deflection simulations with changes of velocity on the order of 0.1 m/s.

C. DEFLECTION RATIO SENSITIVITY TO ORBITAL PARAMETERS

1. Introduction

Since the original simulation program discussed in section B, above, was not satisfactory to test the deflection hypothesis, a simulation program was written in MATLAB which permitted the application of a given change in velocity to a variety of hypothetical asteroid orbits. The MATLAB scripts used are contained in Appendix C. The change in velocity was applied in the plane of the asteroid's orbit. The direction of the change in velocity was applied in five equal increments from along the flight path direction to the anti-flight path direction. As the answers were symmetrically similar, the directional range was altered to five equally spaced inputs from along the flight path to orthogonal to the flight path. These are depicted in Figure 17.

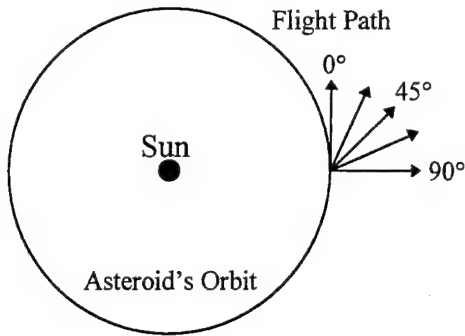


Figure 17. Deflection Directions With Respect to the Flight Path Vector.

2. Variation in Orbital Period for a Circular Orbit

The first sequence of tests applied a 0.135 m/s change in velocity to an asteroid with a circular orbit at 1 AU, inclined to the ecliptic. The Earth's orbit was modeled as a circular orbit in the ecliptic at 1 AU. The simulation calculated the orbital elements of the asteroid's orbits including the true anomaly. From those elements, the eccentric anomaly, mean anomaly, and mean motion were calculated. The orbital velocities at one, two, three, four, five, and ten years prior to collision were calculated, the desired change in velocity applied, and new orbital elements calculated. The entire procedure was then reversed. Finally, the asteroid's position at the original time was determined, compared to the Earth's position, and divided by the Earth's radius to determine a miss ratio in Earth radii. As expected, the asteroid missed by two Earth radii for the flight-path and anti-flight path directions. Results show that the miss ratio decreased by the sine of the angle between the flight path and deflection direction. At 45 deg., the miss ratio decreased to 1.4 Earth radii, while at 90 deg., there was no deviation detected. The magnitude of the deflection distances were symmetric about 90 deg.

3. Constant Radius of Perihelion

To demonstrate the accuracy of the mathematical solution developed in Chapter IV, miss ratios were calculated for an asteroid orbit with a fixed radius of perihelion of 1 AU. Fixing perihelion distance results in varying eccentricity and semi-major axis lengths. Change in miss ratio with change in eccentricity and change in semi-major axis are shown in Figure 18 and Figure 19, respectively. Increasing eccentricity dictates an increase in semi-major axis for a constant radius of perihelion. As such, the two figures look very much the same. As the eccentricity increased from a minimum value of 0.0 to approximately 0.2, the miss ratio increased from 2 Earth radii to approximately 4.2 Earth radii. Over this same variation, the semi-major axis increased from 1 AU to approximately 1.25 AU. As shown in Eqn. (24), the deflection distance varies linearly with the asteroids period. But, because the asteroids period varies with $a^{3/2}$, there is a relatively large increase in miss ratio for increasing values of eccentricity.

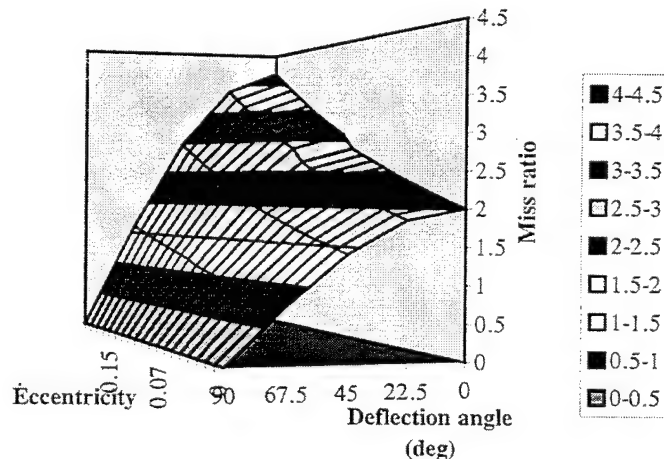


Figure 18. Miss Ratio in Earth Radii vs. Deflection Angle vs. Eccentricity.

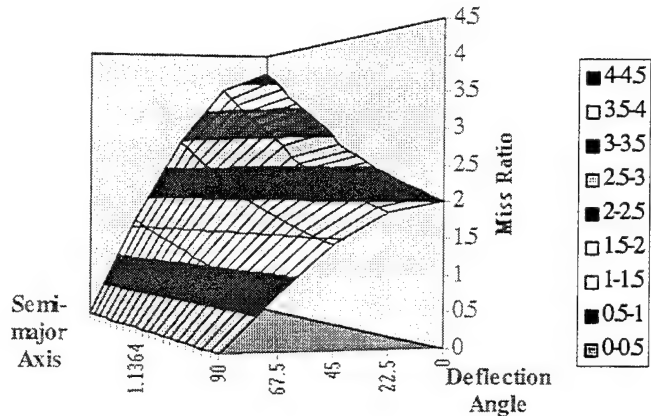


Figure 19. Miss Distance in Earth Radii vs. Deflection Angle vs. Semi-Major Axis.

4. Variation in Eccentricity

The effect of varying the eccentricity of the orbit while maintaining a constant semi-major axis length, shown in Figure 20, provided several interesting results. As the eccentricity increases and a is held constant, the perihelion distance decreases. The line of apsides must then rotate, increasing the true anomaly, to keep the collision distance at 1 AU. The true anomaly increases approximately 5.7 deg. for each 0.1 increase in eccentricity. As the eccentricity increases, the miss distance decreases. The primary cause of this is the application of the change of velocity away from perihelion. The greatest deflections are achieved by applying the change in velocity at perihelion. The least efficient deflections are at aphelion. In this case, the change in velocity is applied approximately 91 deg. past perihelion for eccentricity of 0.01. This increases to approximately 102 deg. past perihelion at $e = 0.2$. The gradient of miss ratio with increase in eccentricity increases significantly beyond $e = 0.2$. This shows the importance of applying a given change in velocity at perihelion.

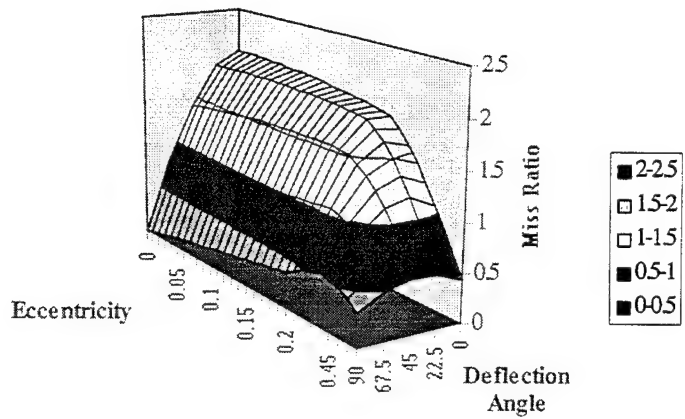


Figure 20. Miss ratio vs. Deflection Angle vs. Semi-Major Axes.

5. Conclusions

The results presented above are consistent with the mathematical conclusions presented in Chapter IV. One of the most important factors in maximizing the miss ratio is targeting the change in velocity to occur at perihelion. This is especially important for high eccentricity orbit with a semi-major axis close to that of the Earth. Much larger changes in velocity are required in these scenarios the further from perihelion the change is to occur.

VI. CONCLUSIONS AND RECOMMENDATIONS

A. SUMMARY

The issues surrounding ECA mitigation necessitate a wide variety of professionals, each with differing areas of expertise, form a project team to formulate the most feasible solution. This paper, for the Naval Postgraduate School and the Space Warfare Center, is the genesis of another small portion of that project team. Although in its infancy, this program, because of the unique composition of its members, can contribute unique and meaningful contributions to that effort.

This paper serves several important purposes. First, it summarizes a few of the important issues involved in planetary defense and serves as a primer to help to gain an understanding of ECAs. Secondly, it serves to develop and analyze the sensitivity of deflection angle and various orbital parameters to miss ratio. Most importantly, it identifies areas for further research and the continuation of this important problem.

Dance of the Planets is not sufficient to serve as a model for the purpose of testing deflection hypotheses. The errors induced into orbital elements or vectors when importing data are of sufficient magnitude to prevent accurate analysis of results. Should the source code become available, increasing the precision used for calculations may solve this problem. This is not to say, however, that the program is without merit. Used as a visualization tool, it provides an extremely flexible and accurate model with which to observe intercept geometry.

The variation of miss ratio with deflection angle, eccentricity, and semi-major axis changes was analyzed. Deflection along the flight path achieve the greatest miss ratios. Position in the orbit also play an important role in the magnitude of the miss ratio. For eccentric orbits, deflection at perihelion is important as miss ratio is fairly sensitive to true anomaly. As true anomaly at deflection increases, the miss ratio decreases. This a

direct result of the deflection being applied at further angular distances from perihelion resulting in less of a change in period for each asteroid orbit.

B. FURTHER RESEARCH OPPORTUNITIES

There are three main areas in the asteroid mitigation problem which would benefit from additional research. First, a complete engineering and mathematical problem formulation should be accomplished. Expanding the scope of the current investigation to include a review of the state-of-the-art in change in velocity delivery options, intercept trajectory optimization, and weapons technology.

Second, asteroid orbit determination accuracy versus the change in velocity required to mitigate a collision should be researched. The accuracy of ephemeris data is extremely important when calculating required changes in velocity and deflection angle. The relationship between the two should be determined to ensure that the proper mitigation steps are taken.

Lastly, the formulation of the sensitivity model developed in this paper should be expanded to include gravitational perturbations and solve the problem using numerical integration techniques. A high fidelity model may provide additional insights into the sensitivity of miss ratio to deflection angle.

LIST OF REFERENCES

1. Morrison, D., editor. 1992. *The Spaceguard Survey: Report of the NASA International Near-Earth-Object Detection Workshop*. (Pasadena: Jet Propulsion Laboratory).
2. Chapman, C. R., Harris, A. W., and Binzel, R. 1994. Physical properties of near-Earth asteroids: Implications for the hazard issue. In *Hazards Due to Comets and Asteroids*, ed. T. Gehrels (Tucson: Univ. of Arizona Press), pp. 537–549.
3. Rahe, J., Vanysek, V., and Weissman, P. R. 1994. Properties of cometary nuclei. In *Hazards Due to Comets and Asteroids*, ed. T. Gehrels (Tucson: Univ. of Arizona Press), pp. 597–634.
4. *Dance of the Planets: A Dynamic Model of the Sky and Solar System*, User's Manual. 1995. Applied Research & Consulting, Inc. (Loveland: Applied Research and Consulting).
5. Rabinowitz, D., Bowell, E., Shoemaker, E. M., and Muinonen, K. 1994. The population of Earth-crossing asteroids. In *Hazards Due to Comets and Asteroids*, ed. T. Gehrels (Tucson: Univ. of Arizona Press), pp. 285–312.
6. Shoemaker, E. M., Williams, J. G., Helin, E. F., and Wolfe, R. F. 1979. Earth-crossing asteroids: Orbital classes, collision rates with Earth, and origin. In *Asteroids*, ed. T. Gehrels (Tucson: Univ. of Arizona Press), pp. 253–282.
7. Shoemaker, E. M., Weissman, P. R., and Shoemaker, C. S. 1994. The flux of periodic comets near the Earth. In *Hazards Due to Comets and Asteroids*, ed. T. Gehrels (Tucson: Univ. of Arizona Press), pp. 313–335.

8. Helin, E. F. 1982. Earth-crossing asteroids: New discoveries. In *Sun and Planetary System*. ed. G. Teleki (D. Reidel Publishing Company), pp. 269–276.
9. Simonenko, V. A., Nogin, V. N., Petrov, D. N., Shubin, O. N., and Solem, J. C. 1994. Defending the Earth Against Impacts From Comets and Asteroids. In *Hazards Due to Comets and Asteroids*, ed. T. Gehrels (Tucson: Univ. of Arizona Press), pp. 929–953.
10. Bate, R. R., Mueller, D. D., and White, J. E. 1971. *Fundamentals of Astrodynamics*. (New York: Dover Publications).
11. Wertz, J. R. 1978. Editor, *Spacecraft Attitude Determination and Control*. Boston: Kluwer Academic Publishers.
12. Canavan, G. H., Solem, J. C., Rather, J. D. C., eds. 1993. *Proceedings of the Near-Earth-Object Interception Workshop*. (Los Alamos: Los Alamos National Laboratory).
13. Shoemaker, E. M., and Helin, E. F. 1978. Earth-approaching asteroids: Populations, origin and compositional types. NASA Conf. Public. 2053, pp. 161–175.

APPENDIX. MATLAB SCRIPT FILES

This appendix contains the MATLAB function files constructed during the research of the asteroid mitigation problem. Section I contains the scripts which calculate a hypothetical asteroid's position and velocity vectors based on the current position and velocity of the Earth. `Demo.m` calculates all data by accessing individual script files. In `Demo.m` the user inputs the Earth's position and velocity vectors, `r1` and `v1`, respectively. Position is in 1E6 km and velocity is in km/sec. For an elliptical orbit, the user inputs into `elip.m` the desired semimajor axis length, eccentricity, and inclination. For a parabolic orbit, the user inputs into `parab.m` the desired semi-latus rectum, and inclination. Hyperbolic orbit script files were not developed. When `demo.m` is executed, available outputs include the asteroid's position and velocity vectors in heliocentric ecliptic coordinates and the asteroid's orbital elements. Current position in the orbit is output as true anomaly.

Section 2 calculates the miss ratio, the ratio of the difference between the Earth's position and the asteroid's position one asteroid orbit following the imparted change in velocity to the radius of the Earth. The user inputs the Earth's position and velocity vectors, as discussed above, into `Demo1.m`. The user also inputs into `demo.m` the magnitude of the change in velocity to be applied, normalized for one orbit, and the number of orbits prior to collision the change in velocity is to be applied. In `elip1.m` the user inputs are the desired semi-major axis, eccentricity, inclination for asteroid at the time of Earth impact. The program then calculates the remaining orbital parameters for the asteroid's orbit. From these, the eccentric anomaly, mean anomaly, and mean motion are found and used to find the asteroid's position at some specified number of asteroid orbits prior to collision. The change in velocity is then applied in five 22.5 deg. increments from along the flight path to 90 deg. to the flight path. New values for mean motion, mean anomaly, and eccentric anomaly are found and the new position obtained at the original time. The miss ratio is then calculated to determine how many Earth radii the new position differs from the old position. Outputs include new velocity vectors, orbital elements, true anomaly, and miss ratio for each of the five directions.

Summary of function files:

trun anom: True anomaly determination from r,v,e,n.
 incl: Inclination determination from h.
 lan: Long. of Ascending Node determination from n.
 aop: Argument of Perihelion determination from n,e,r.
 rot: Rotation matrix from perifocal to HCl. Inputs are Omega,i,omega.
 elip: Finds r,v,nu,dcm from Earth's rmag,dcm,nu.
 parabola: Finds r,v,nu,dcm from Earth's rmag,dcm,nu.
 earthorb: Calculates Earth's r vector in perifocal and HCl from a,ecc,dcm.
 cx,cy,cz: Compute a single axis direction cosine matrix.
 tlop: Compute true longitude of perihelion from e.
 deltav: Computes the new velocity vector components after the delta v is imparted to the asteroid.
 elements: Returns the matrix sets of:
 el_prev: orbital elements prior to deflection.
 el_next: orbital elements after deflection.
 rv_next: position and velocity vectors at original impact time.
 elip1: Computes the asteroid's orbit given the Earth's rmag,dcm,nu and user defined values for a,e,i.
 elip2: Computes the asteroid's new r,v given the asteroid's position at deflection, r, the dcm from the orbital elements, the position in the old orbit, ecc_a,a_a.
 function1/2: Solve Kepler's equation for E.
 param: Given r,v returns a,ecc,Omega,incl,omega,nu,E,M,dcm,rmag.

Variables:

_ma
 r: Position vector.
 v: Velocity vector.
 e: Eccentricity vector.
 n: Node vector.
 h: Angular momentum vector.
 Omega: Longitude of the ascending node.
 i: Inclination.
 omega: Argument of perihelion.
 dcm: Direction cosine matrix from perifocal to heliocentric-ecliptic coordinate system for Earth's orbit.
 nu: True anomaly.
 a: Semi-major axis.
 ecc: Eccentricity.
 dcm2: Direction cosine matrix from perifocal to heliocentric-ecliptic coordinate system for asteroid's orbit.

$*_e$	Earth variable.
$*_a$	Asteroid variable.
$*_{old}$	Asteroid variable at time of impact.
$*_{prev}$	Asteroid variable at some time prior to impact.
$*_{new}$	Asteroid variable just after application of change in velocity.
$*_{next}$	Asteroid variable in new orbit but at time of original impact.
p	Semi-latus rectum.
r_p	Perihelion distance.
r_a	Aphelion distance.
E	Eccentric anomaly.
M	Mean anomaly.
n	Mean motion.

I. ORBIT DETERMINATION AND GRAPHING SCRIPTS

A. CALCULATE AND PLOT ORBITS: FILE ENTITLED DEMO.M

```
% Given: The Earth's position and velocity vectors.
% First: Calculate the Earth's orbital elements.
% Second: Plot the Earth's orbit wrt the mean ecliptic.
% Third: Choose the type of assailant object orbit:
% a. Circular or elliptical
% b. Parabolic
% c. Hyperbolic
% Fourth: Choose the desired values for:
% a. Semi-major axis or parameter
% b. Eccentricity
% c. New inclination with respect to Earth's inclination.

clear

% Constants
rtd=180/pi; % Radians to degrees
dtr=1/rtd; % Degrees to radians
I = [1 0 0]; % Unit vectors
J = [0 1 0];
K = [0 0 1];
AU = 1.4959965e8; % km
TU = 5.0226757e6; % sec
SU = 29.784852; % km/sec
mu = 1; % km^3/sec^2

% Earth values:
r1=[-26 144.8 -.00038]; % Position
v1=[-29.8 -5.376 -.000043]; % Velocity

r=r1*1e6/AU;
v=v1/SU;
rmag=norm(r);
vmag=norm(v);

% angular momentum
h=cross(r,v);
hmag=norm(h);

% eccentricity vector
e=cross(v,h)-r/rmag;
ecc=norm(e);

if ecc<1e-10, % Check if eccentricity is zero
e = [0 0 0];
ecc=0;
```

```

    end

% node vector
n = cross(K,h);
nmag=norm(n);

if nmag<1e-10,    % Check if inclination is zero
    n = [0 0 0];
    nmag=0;
end

% Find the true anomaly at epoch
nu = truanom(r,v,e,n);

% Compute the inclination
inc = incl(h)

% Compute the longitude of ascending node
Omega=lan(n)

% Compute the argument of perigee
omega = aop(n,e,r)

% Compute the rotation matrix
dcm=rot(Omega,inc,omega);

% Determine if user wants another orbit calculated
plt = input('Do you want to calculate a new orbit? y/n [y]:','s');

if isempty(plt)
    plt = 'y';
end

if plt == 'y',
% *****
% choose an a,e for orbit and solve for nu_2 for the new orbit

fprintf('\nYou may now calculate a new intercept orbit type.\n');

type = input('Do you want to plot an Ellipse, Parabola, or Hyperbola? e/p/h
[e]:','s');
if isempty(type)
    type = 'e';
end

if type == 'e',    % Eliptical/Circular Plot
    [r_new,v_new,nu_new,dcm2]=elip(rmag,dcm,nu);

elseif type == 'p',    % Parabolic Orbit Plot
    [r_new,v_new,nu_new]=parabola(rmag,dcm,nu);

elseif type == 'h',    % Hyperbolic Orbit Plot
    [r_new,v_new,nu_new]=hyperb(rmag,dcm,nu)

```

```

    end % end plotting of second orbit

r_old = r1
r_new = r_new * AU/1e6
v_old = v1
v_new = v_new*SU
del_v = abs(norm(v_old-v_new))

end

% Calculate the Earth's orbit
p = hmag^2/mu; % semilatus rectum
a = p/(1-ecc^2); % semimajor axis
rp = p/(1+ecc); % perigee
ra = p/(1-ecc); % appogee
[x,y,z,xx,yy,zz]=earthorb(a,ecc,dcm);

% Plot the Earth's orbit with respect to the ecliptic
hold on;
plot3(xx,yy,zz,'m'); % orbit

xyz_r=r; % position
plot3(xyz_r(1),xyz_r(2),xyz_r(3),'g+');

if type == 'e', % Eliptical/Circular Plot
    legend('b','Asteroid''s
orbit','or','Perihelion','*r','Aphelion','+g','Current Position',...
'm','Earth''s orbit')

elseif type == 'p' | 'h', % Parabolic Orbit Plot
    legend('b','Asteroid''s orbit','or','Perihelion','+g','Current
Position',...
'm','Earth''s orbit')
end

xyz_per=dcm*[rp;0;0]; % perihelion
plot3(xyz_per(1),xyz_per(2),xyz_per(3),'mo');

xyz_apo=dcm*[-ra;0;0]; % aphelion
plot3(xyz_apo(1),xyz_apo(2),xyz_apo(3),'m*');

% end plotting of second orbit

% Axis plotting statements.

l=2;
ds=.2;
A=[0 0 0;1 0 0];
B=[0 0 0;0 1 0];
C=[0 0 0;0 0 1];
plot3(A,B,C,'w');
text(l+ds,0,0,'X','horizontalalignment','center');
text(0,l+ds,0,'Y','horizontalalignment','center');

```

```

text(0,0,1+ds,'Z','horizontalalignment','center');
view(viewmtx(135,30,25));
title('General View');
axis('square');axis off;
axis([-a,a,-a,a,-a,a]);
end;

% View radio buttons
txt_view=uicontrol(gcf, ...
    'Style','text',...
    'String','Asteroid Orbit View',...
    'Units','normalized',...
    'Position',[.05,.87,.20,.03]);
view_gen=uicontrol(gcf, ...
    'Style','radio',...
    'String','Standard',...
    'Units','normalized',...
    'Position',[.05,.80,.20,.05],...
    'Value',1,...
    'CallBack',[...
    'title('''General View'''),'...
    'set(view_gen,''Value'',1),',...
    'set(view_x,''Value'',0),',...
    'set(view_y,''Value'',0),',...
    'set(view_z,''Value'',0),',...
    'set(view_n,''Value'',0),',...
    'view(135,30)']);
view_x=uicontrol(gcf, ...
    'Style','radio',...
    'String','Down X Axis',...
    'Units','normalized',...
    'Position',[.05,.75,.20,.05],...
    'CallBack',[...
    'title('''View Looking Down +X axis'''),'...
    'set(view_gen,''Value'',0),',...
    'set(view_x,''Value'',1),',...
    'set(view_y,''Value'',0),',...
    'set(view_z,''Value'',0),',...
    'set(view_n,''Value'',0),',...
    'view([1,0,0])']);
view_y=uicontrol(gcf, ...
    'Style','radio',...
    'String','Down Y Axis',...
    'Units','normalized',...
    'Position',[.05,.70,.20,.05],...
    'CallBack',[...
    'title('''View Looking Down +Y axis'''),'...
    'set(view_gen,''Value'',0),',...
    'set(view_x,''Value'',0),',...
    'set(view_y,''Value'',1),',...
    'set(view_z,''Value'',0),',...
    'set(view_n,''Value'',0),',...
    'view([0,1,0])']);

```

```

view_z=uicontrol(gcf, ...
    'Style','radio',...
    'String','Down Z Axis',...
    'Units','normalized',...
    'Position',[.05,.65,.20,.05],...
    'CallBack',[...
        'title('''View Looking Down +Z axis'''),'...
        'set(view_gen,''Value'',0),',...
        'set(view_x,''Value'',0),',...
        'set(view_y,''Value'',0),',...
        'set(view_z,''Value'',1),',...
        'set(view_n,''Value'',0),',...
        'view([0,0,1]))');

xyz_norm=dcm2*[0;0;1];
view_n=uicontrol(gcf, ...
    'Style','radio',...
    'String','Down Orbit Normal',...
    'Units','normalized',...
    'Position',[.05,.60,.20,.05],...
    'CallBack',[...
        'title('''View Looking Down Orbit Normal'''),'...
        'set(view_gen,''Value'',0),',...
        'set(view_x,''Value'',0),',...
        'set(view_y,''Value'',0),',...
        'set(view_z,''Value'',0),',...
        'set(view_n,''Value'',1),',...
        'view([xyz_norm(1),xyz_norm(2),xyz_norm(3)])']);
    ]);

% Zoom Slider
zoom=uicontrol(gcf, ...
    'Style','slider',...
    'Units','normalized',...
    'Position',[.05,.15,.20,.05],...
    'Min',.5,'Max',5.5,'Value',1,...
    'CallBack',[...
        'set(zoom_cur,''String'',num2str(get(zoom,''Val''))),',...
        'set(gca,''Xlim'',[-
    get(zoom,''Value''),get(zoom,''Value'')]'),',...
        ''''Ylim'',[-get(zoom,''Value''),get(zoom,''Value'')]'),',...
        ''''Zlim'',[-get(zoom,''Value''),get(zoom,''Value'')]])');
    ]);

zoom_label=uicontrol(gcf, ...
    'Style','text',...
    'Units','normalized',...
    'Position',[.05,.205,.20,.03],...
    'String','Zoom');

zoom_cur=uicontrol(gcf, ...
    'Style','text',...
    'Units','normalized',...
    'Position',[.095,.115,.11,.03],...
    'String',num2str(get(zoom,'Value')));

zoom_in=uicontrol(gcf, ...
    'Style','text',...
    'Units','normalized');

```

```

'Position',[.05,.115,.04,.03],...
'String','In');
zoom_out=uicontrol(gcf,...
'Style','text',...
'Units','normalized',...
'Position',[.21,.115,.04,.03],...
'String','Out');

% Print push button
prt

```

B. AOP

```

%-----*
% Calculation of the argument of
% perigee, in degrees
%
% LCDR Wade Knudson
% Naval Postgraduate School
% Orbit Visualization Routines
%
% Inputs: n,e,r
%
% Output: omega
%
% Files called: tlop
%
% [omega] = aop(n,e,r)
%-----*

```

C. ARGUMENT OF PERIHELION

```

function [omega] = aop(n,e,r)

nmag=norm(n);
ecc=norm(e);
rmag=norm(r);
I = [1 0 0];
J = [0 1 0];
K = [0 0 1];
rtd=180/pi;

% Check to see if the orbit is circular (e=0) and in the ecliptic (n=0);
% if so, then omega is not used; use true longitude at epoch (Vallado p.
139)

if nmag == 0 & ecc == 0,
    omega = 0;

```

```

% Check to see if the orbit is elliptical (e>0) and in the ecliptic (n=0);
% if so, then omega is not used; use true longitude of periapsis (Vallado
p. 136)

elseif nmag == 0 & ecc ~=0,
    om_true = tlop(e);
    %fprintf('This is an elliptical orbit in the ecliptic.\n')
    %fprintf('The inclination is zero.\n')
    %fprintf('\n')
    %fprintf('The angle between Aries and periapsis is called \n')
    %fprintf('the true longitude of periapsis, and is %3.1f
deg.\n',om_true)
    omega = om_true;

% Check to see if the orbit is a circular (e=0) and inclined to the
ecliptic
elseif nmag ~= 0 & ecc == 0,
    if dot(r,K)<0,
        omega = 360 - acos(dot(n,r)/(nmag*rmag))*rtd;
    else
        omega = acos(dot(n,r)/(nmag*rmag))*rtd;
    end

% All remaining cases
else
    if dot(e,K) < 0,
        omega = 360 - acos(dot(n,e)/(nmag*ecc))*rtd;
    else
        omega = acos(dot(n,e)/(nmag*ecc))*rtd;
    end
end

```

D. CX

```

function f=cx(angle)

f=[1 0 0; 0 cos(angle) sin(angle); 0 -sin(angle) cos(angle)];

```

E. CY

```

function f=cy(angle)

f=[cos(angle) 0 -sin(angle); 0 1 0; sin(angle) 0 cos(angle)];

```

F. CZ

```

function f=cz(angle)

f=[cos(angle) sin(angle) 0; -sin(angle) cos(angle) 0; 0 0 1];

```

G. EARTH ORB

```
%-----  
%  
% Calculation of the Earth's orbit  
%  
%  
% LCDR Wade Knudson  
% Naval Postgraduate School  
% Orbit Visualization Routines  
%  
% Inputs: a,ecc,dcm  
%  
% Output: x,y,z: perifocal coordinates  
% xx,yy,zz: heliocentric coordinates  
%  
% Files called: None  
%  
% [x,y,z,xx,yy,zz] = earthorb(a,ecc,dcm)  
%-----  
  
function [x,y,z,xx,yy,zz] = earthorb(a,ecc,dcm)  
  
m=400;  
E=linspace(0,2*pi,m);  
x=-a*ecc+a*cos(E);y=a*sqrt(1-ecc^2)*sin(E); %Battin p. 158  
z=zeros(1,m);  
for k=1:m  
    point=dcm*[x(k);y(k);z(k)];  
    xx(k)=point(1);yy(k)=point(2);zz(k)=point(3);  
end;
```

H. ELIPTICAL ORBIT CALCULATIONS

```
%-----  
%  
% Calculation of the Elliptical/circular orbit  
%  
%  
% LCDR Wade Knudson  
% Naval Postgraduate School  
% Orbit Visualization Routines  
%  
% Inputs: rmag,dcm,nu  
%  
% User inputs: a,ecc,incl  
%  
% Output: r,v, and nu for the new orbit  
%  
% Files called: cx,cz  
%-----
```

```

%      [r,v,nu_new] = elip(rmag,dcm,nu)          *
%
%-----

function [r,v,nu_new,dcm2] = elip(rmag,dcm,nu)

% Constants
rtd = 180/pi;
dtr = 1/rtd;
mu = 1;

%a = input('Type in the semi-major axis')

% If ecc == 0, then 'a' must equal rmag.
% If ecc ~= 0, then rp < a < ra.
a=2.032;
ecc=.651;
newinc=5.46;

if ecc == 0,                         % If circular then no
% rotation to argument
    nu_new = 0;                      % of periapsis (nu_new)
    a = rmag;
    p = a;
else
    p =a*(1-ecc^2);
    nu_new=acos((p/rmag-1)/ecc)*rtd;    % true anomaly
end

rp = p/(1+ecc);                     % periapsis
ra = p/(1-ecc);                     % apoapsis

% Perifocal coordinates
r = [rmag*cos(nu_new*dtr) rmag*sin(nu_new*dtr) 0];
v = sqrt(mu/p)*[-sin(nu_new*dtr) ecc+cos(nu_new*dtr) 0];

% rotate the new orbit to the line of node (-nu), then to desired
% inclination,
% and finally rotate nu_2 to get epoch to r.

% Asteroid's dcm matrix
dcm2= dcm*cz(-nu*dtr)*cx(-newinc*dtr)*cz(nu_new*dtr);

m=200;
E=linspace(0,2*pi,m);
x=-a*ecc+a*cos(E);
y=a*sqrt(1-ecc^2)*sin(E); % Battin p. 158
z=zeros(1,m);
for k=1:m
    point=dcm*[x(k);y(k);z(k)];
    xx(k)=point(1);yy(k)=point(2);zz(k)=point(3);
    point2=dcm2*[x(k);y(k);z(k)];
    xxx(k)=point2(1);yyy(k)=point2(2);zzz(k)=point2(3);

```

```

    end

% Plot the asteroid's new orbit
    hold on;

    plot3(xxx,yyy,zzz,'b'); % orbit

    xyz_per=dcm2*[rp;0;0]; % perihelion
    plot3(xyz_per(1),xyz_per(2),xyz_per(3),'bo');

    xyz_apo=dcm2*[-ra;0;0]; % aphelion
    plot3(xyz_apo(1),xyz_apo(2),xyz_apo(3),'b*');

    xyz_r=(dcm2*r)'; % position
    % rvector
    plot3(xyz_r(1),xyz_r(2),xyz_r(3),'g+');

    legend('Asteroid''s orbit','Perihelion','Aphelion')

% Calculate the new r,v vectors
    r = xyz_r;
    v = (dcm2*v)';

```

I. INCLINATION

```

%-----*
% Calculation of the inclination in degrees
%
%
% LCDR Wade Knudson
% Naval Postgraduate School
% Orbit Visualization Routines
%
% Inputs: h
%
% Output: inc
%
% Files called: none
%
% [inc] = inc(h)
%
%-----*

```

```

function inc = inc(h)

K=[0 0 1];
rtd=180/pi;
hmag=norm(h);

inc = acos(dot(h,K)/hmag)*rtd;

```

J. LONGITUDE OF ASCENDING NODE

```
%-----  
% Calculation of the longitude of  
% the ascending node, in degrees  
%  
% LCDR Wade Knudson  
% Naval Postgraduate School  
% Orbit Visualization Routines  
%  
% Inputs: n  
%  
% Output: Omega  
%  
% Files called: none  
%  
% [Omega] = lan(n)  
%-----  
function [Omega] = lan(n)  
  
nmag=norm(n);  
I = [1 0 0];  
J = [0 1 0];  
rtd=180/pi;  
  
if nmag == 0, % Provides check for inclination  
    Omega = 0; % If no inclination then no Omega  
  
else % If some inclination then  
    % find Omega  
    if dot(n,J) < 0,  
        Omega = 360 - acos(dot(n,I)/nmag)*rtd;  
    else  
        Omega = acos(dot(n,I)/nmag)*rtd;  
    end  
  
end
```

K. PARABOLA

```
%-----  
% 3-D plot of the parabolic orbit which intercepts  
% the Earth's position at a given time  
%  
% LCDR Wade Knudson  
% Naval Postgraduate School  
% Orbit Visualization Routines  
%  
% Inputs: rmag,dcm,nu  
% User input: p,incl  
%  
% Output: r,v, and nu for the new orbit  
%-----
```

```

%
%      Files called:  cx,cz
%
%      [r,v,nu_new] = parabola(rmag,dcm,nu)
%
%-----
```

function [r,v,nu_new] = parabola(rmag,dcm,nu)

% Constants

```

rtd = 180/pi;
dtr = 1/rtd;
mu = 1;
```

p=1.9;
newinc=90;

ecc=1;

nu_new=acos((p/rmag-1)/ecc)*rtd; % true anomaly

rp = p/(1+ecc) % perihelion

% Perifocal Coordinates

```

r = [rmag*cos(nu_new*dtr) rmag*sin(nu_new*dtr) 0];
v = sqrt(mu/p)*[-sin(nu_new*dtr) ecc+cos(nu_new*dtr) 0];
```

% rotate the new orbit to the line of node (-nu), then to desired inclination,
% and finally rotate nu_2 to get epoch to r.

```

dcm2= dcm*cz(-nu*dtr)*cx(-newinc*dtr)*cz(nu_new*dtr);
```

m=200;
f=linspace(-pi+.1,pi-.1,m);
x1 = (p*cos(f));y1 = (p*sin(f));
x2 = (1+cos(f));y2 = (1+cos(f));

x = x1./x2;y = y1./y2; % Battin p. 158
z=zeros(1,m);

for k=1:m
 point=dcm*[x(k);y(k);z(k)];
 xx(k)=point(1);yy(k)=point(2);zz(k)=point(3);
 point2=dcm2*[x(k); y(k); z(k)];
 xxx(k)=point2(1);yyy(k)=point2(2);zzz(k)=point2(3);
end

% Plot the asteroid's new orbit
hold on;

```

plot3(xxx,yyy,zzz,'b');                                % orbit

xyz_per=dcm2*[rp;0;0];                                % perihelion
plot3(xyz_per(1),xyz_per(2),xyz_per(3),'bo');

xyz_r=(dcm2*r')';                                     % position
% rvector
plot3(xyz_r(1),xyz_r(2),xyz_r(3),'g+');

% Calculate the new r,v vectors and orbital elements.
r = xyz_r
v = (dcm2*v')'

```

L. PRINT

```

% Puts a print push button on a figure.
function prnbut = prt
    prt=uicontrol(gcf,...
        'Style','push',...
        'Units','normalized',...
        'Position',[.05,.02,.20,.05],...
        'String','Print',...
        'CallBack','print');

```

M. ROTATION DCM

```

%-----*
%
% Calculation of the rotation matrices for a 3-1-3           *
% rotation to convert from perifocal coordinates to           *
% heliocentric-ecliptic                                     *
%
% LCDR Wade Knudson                                         *
% Naval Postgraduate School                                    *
% Orbit Visualization Routines                                *
%
% Inputs: Omega,inc,omega                                     *
%
% Output: dcm                                              *
%
% Files called: cx,cz                                         *
%
% [dcm] = rotmat(Omega,inc,omega)                            *
%
%-----*

```

```

function [dcm] = rot(Omega,inc,omega)

dtr=pi/180;

O=Omega*dtr;
i=inc*dtr;

```

```

o=omega*dtr;
dcm = cz(-O)*cx(-i)*cz(-o);

```

N. TRUE LONGITUDE OF PERIHELION

```

%-----*
%
% True longitude of periapsis *
% Used for elliptical orbits in the reference plane *
%
% LCDR Wade Knudson *
% Naval Postgraduate School *
% Orbit Visualization Routines *
%
% Inputs: e *
%
% Output: True longitude of periapsis *
%
% Files called: none *
%
% [om_true] = tlop(e) *
%
%-----*

```

```

function om_true = tlop(e)

rtd = 180/pi;
I = [1 0 0];
J = [0 1 0];
emag = norm(e);

if dot(J,e) < 0,
    om_true = 360 - acos(dot(I,e)/emag)*rtd;
else
    om_true = acos(dot(I,e)/emag)*rtd;
end

```

O. TRUE ANOMALY

```

%-----*
%
% Calculation of the true anomaly at epoch, in degrees *
%
% LCDR Wade Knudson *
% Naval Postgraduate School *
% Orbit Visualization Routines *
%
% Inputs: r,v,e *
%
% Output: nu *
%
% Files called: none *
%
%-----*

```

```

%      [nu] = truanom(r,v,e,n)                                *
%      *                                                 *
%-----

function [nu] = truanom(r,v,e,n)

rmag=norm(r);
nmag=norm(n);
ecc=norm(e);
rmag=norm(r);
I = [1 0 0];
J = [0 1 0];
K = [0 0 1];
rtd=180/pi;

% First check for circular orbit in the ecliptic. If not, skip.
if ecc == 0 & n == 0,
    if dot(J,r)<0,
        lamda_t = 360 - acos(dot(I,r)/rmag)*rtd;
    else
        lamda_t = acos(dot(I,r)/rmag)*rtd;
    end

nu = lamda_t;
fprintf('This is a circular orbit in the ecliptic. \n')
fprintf('The longitude of ascending node is undefined.\n')
fprintf('The inclination is zero.\n')
fprintf('\n')
fprintf('The angle between aries and the position of the body\n')
fprintf('is called the true longitude at epoch, and is %3.1f deg.\n',nu)

% Next check for circular inclined orbit. If not, skip.
elseif ecc == 0 & nmag ~= 0,

    if dot(r,K)<0,
        u = 360 - acos(dot(n,r)/(nmag*rmag))*rtd;
    else
        u = acos(dot(n,r)/(nmag*rmag))*rtd;
    end

nu = u;
fprintf('This is a circular, inclined orbit. \n')
fprintf('\n')
fprintf('The argument of perigee is known as the \n')
fprintf('argument of latitude at epoch, and is %3.1f deg.\n',u)

else
    if dot(r,v) < 0,
        [nu] = 360 - acos(dot(e,r)/(ecc*rmag))*rtd;
    else
        [nu] = acos(dot(e,r)/(ecc*rmag))*rtd;
    end
    fprintf('This is an elliptical orbit. \n')

```

```
if nmag == 0 & ecc ~= 0,
    %fprintf('The orbit is in the ecliptic.\n')
else
    %fprintf('The orbit is inclined to the ecliptic.\n')
end
%fprintf('\n')
%fprintf('The true anomaly at epoch is %3.1f deg.\n',nu)

end
```

II. SENSITIVITY SCRIPTS

A. MISS RATIO CALCULATIONS: DEMO1

```
clear all
rtd=180/pi;
dtr=1/rtd;
I = [1 0 0];
J = [0 1 0];
K = [0 0 1];
AU = 1.4959965e8; % km
TU = 5.0226757e6; % sec
SU = 29.784852; % km/sec
mu = 1; % km^3/sec^2

%r=[-26 144.8 -.00038];
%v=[-29.8 -5.376 -0.000043];

r=[AU 0 0]/1e6;
v=[0 SU 0];
num_orbs = 1;

% Calculate the orbital elements for the Earth from the r/v vectors;
% Input are the position and velocity vectors
% Outputs are shown:
[a_e,ecc_e,O_e,inc_e,o_e,nu_e,E_e,M_e,dcm_e,rmag_e] = param(r,v);

%
% choose an a,e for orbit and solve for nu_2 for the new orbit

% Determine if user wants another orbit calculated
%plt = input('Do you want to calculate a new orbit? y/n [y]:','s');

%if isempty(plt)
%    plt = 'y';
%end

if plt == 'y',
    %fprintf('\nYou may now calculate a new intercept orbit type.\n');

    %type = input('Do you want to plot an Ellipse, Parabola, or Hyperbola?
    %e/p/h [e]?:','s');
    %if isempty(type)
    %    type = 'e';
    %end
%
```

```

% ^^^^^^^^^^^^^^^^^^^^^^^^^^^^^^^^^^^^^^^^^^^^^^^^^^^^^^^^^

% Calculate new r/v vectors based on inputting desired values of
% a,e,inc. Omega,omega, and nu are not variables, but fixed, based
% on the Earth's orbit.

if type == 'e', % Elliptical/Circular Plot
    [r_new,v_new,nu_new,dcm2,ecc]=elip1(rmag_e,dcm_e,nu_e);

elseif type == 'p', % Parabolic Orbit Plot
    [r_new,v_new,nu_new]=parabola(rmag,dcm,nu)

elseif type == 'h', % Hyperbolic Orbit Plot
    [r_new,v_new,nu_new]=hyperb(rmag,dcm,nu)

end % end plotting of second orbit

% Compute the orbital parameters of the new orbit:
global compare
[a_a,ecc_a,O_a,inc_a,o_a,nu_a,E_a,M_a,dcm_a,rmag_a] = param(r_new,v_new);

% Compute the period of the asteroid's orbit
mu_s = 1;
TP = 2*pi*(a_a)^1.5/sqrt(mu_s)*TU/3600/24/365.25; % In Earth years

% Input here how many asteroid orbits to go through. You should go through
% at least one asteroid orbital period to ensure sufficient time for
deflection.
n_a= sqrt(mu_s/a_a^3); % mean motion
t=-TP*num_orbs*365.25*24*3600/TU; % convert years to canonical
global t

% Compute the required delta V required along the flight path
del_tot=0.000135/num_orbs;

% Compute mean anomaly for some past time.
M_prev = M_a + n_a*t;
M_prev1 = M_prev - fix(M_prev/2/pi)*2*pi + 2*pi;
global M_prev ecc_a

% Previous eccentric anomaly
E_prev = fzero('fun',M_prev);

% Compute previous true anomaly
nu_prev = acos((ecc_a-cos(E_prev))/(ecc_a*cos(E_prev)-1))*rtd;

% Compute rmag for previous time
rmag_prev = a_a*(1-ecc_a*cos(E_prev));

% Compute the r/v at the previous time

```

```

[r_prev v_prev]=elip2(rmag_prev,dcm_a,nu_prev,ecc_a,a_a);

%[a_a_p,ecc_a_p,O_a_p,inc_a_p,o_a_p,nu_a_p,E_a_p,M_a_p,dcm_a_p] =
param(r_prev,v_prev);

% Compute the new matrix of delta_v's
[el_prev el_next rv_next]=deltav(r_prev,v_prev,del_tot,nu_new);

delta_rv=zeros(6,6);
for s=1:6
    delta_rv(s,1:3) = (r_e - rv_next(s,1:3))*1e6;
    delta_rv(s,4:6) = v_prev - rv_next(s,4:6);
    mag_del_rv(s,:) = [norm(delta_rv(s,1:3)) norm(delta_rv(s,4:6))];
end

time_ratio=[nu_new a_a ecc_a (mag_del_rv(2:6,1)/6378.145)'];
fprintf('\n      nu      a      e      0.0      22.5      45      67.5
90\n');
fprintf('\n
%7.4f%7.4f%7.4f%7.4f%7.4f%7.4f%7.4f%7.4f%7.4f\n\n', [time_ratio]);
fprintf('\n');
keyboard

```

B. DELTA V DETERMINATION

```

function [el_prev,el_next,rv_next] = deltav(r1,v1,dv_tot,nu_new)

% Constants
rtd=180/pi;
dtr=1/rtd;
I = [1 0 0];
J = [0 1 0];
K = [0 0 1];
AU = 1.4959965e8; % km
TU = 5.0226757e6; % sec
SU = 29.784852; % km/sec
mu = 1; % km^3/sec^2

% Orbit values:
r=r1*1e6/AU;
v=v1/SU;
rmag=norm(r);
vmag=norm(v);

% angular momentum
h=cross(r,v);
hmag=norm(h);

% eccentricity vector
e=cross(v,h)-r/rmag;
ecc=norm(e);
if ecc<1e-10, % Check if eccentricity is zero
    e = [0 0 0];

```

```

        ecc=0;
    end

    % node vector
    n = cross(K,h);
    nmag=norm(n);
    if nmag<1e-10,                                % Check if inclination is zero
        n = [0 0 0];
        nmag=0;
    end

    % Find the true anomaly at epoch
    nu = truanom(r,v,e,n);

    % Compute the inclination
    inc = incl(h);

    % Compute the longitude of ascending node
    Omega=lan(n);

    % Compute the argument of perigee
    omega = aop(n,e,r);

    % Compute the rotation matrix
    dcm=rot(Omega,inc,omega);

    direct=linspace(pi/2,0,5);
    x=cos(direct); y=sin(direct);
    z=zeros(1,5);

    for k = 1:5,
        dv=[x(k) y(k) z(k)];

        if abs(x(k))<1e-12
            x(k)=0;
        end

        if abs(y(k))<1e-12
            y(k)=0;
        end

        if abs(z(k))<1e-12
            z(k)=0;
        end
    end

    z=zeros(1,5);
    epoch=0;

    dv1 = (dv_tot*[x(1) y(1) z(1)]');
    dv2 = (dv_tot*[x(2) y(2) z(2)]');
    dv3 = (dv_tot*[x(3) y(3) z(3)]');

```

```

dv4 = (dv_tot*[x(4) y(4) z(4)]');
dv5 = (dv_tot*[x(5) y(5) z(5)]');

rot = cz(nu_new*dtr);

vnew_1 = (rot*(v1 + dv1'))';
vnew_2 = (rot*(v1 + dv2'))';
vnew_3 = (rot*(v1 + dv3'))';
vnew_4 = (rot*(v1 + dv4'))';
vnew_5 = (rot*(v1 + dv5'))';

% Print the old position and velocity vectors and the new velocity
vectors

r_prev = r1;
v_prev = v1;
dv = [v_prev;vnew_1;vnew_2;vnew_3;vnew_4;vnew_5];

%fid=fopen('new_orb.vec','w');
%fprintf(fid,'ObjVectors x y z vx vy
%vz epoch\n');
%fprintf(fid,'%6.0f%11.5f%11.5f%11.5f%10.6f%10.6f%10.6f%11.4f\n',[0 r_prev
vz epoch]);
%fprintf(fid,'%6.0f%11.5f%11.5f%11.5f%10.6f%10.6f%10.6f%11.4f\n',[1 r_prev
vnew_1 epoch]);
%fprintf(fid,'%6.0f%11.5f%11.5f%11.5f%10.6f%10.6f%10.6f%11.4f\n',[2 r_prev
vnew_2 epoch]);
%fprintf(fid,'%6.0f%11.5f%11.5f%11.5f%10.6f%10.6f%10.6f%11.4f\n',[3 r_prev
vnew_3 epoch]);
%fprintf(fid,'%6.0f%11.5f%11.5f%11.5f%10.6f%10.6f%10.6f%11.4f\n',[4 r_prev
vnew_4 epoch]);
%fprintf(fid,'%6.0f%11.5f%11.5f%11.5f%10.6f%10.6f%10.6f%11.4f\n',[5 r_prev
vnew_5 epoch]);

%fprintf('
ObjVectors x y z vx vy
vz \n');
%fprintf('%6.0f%11.5f%11.5f%11.5f%10.6f%10.6f%10.6f\n',[0 r_prev v_prev ]);
%fprintf('%6.0f%11.5f%11.5f%11.5f%10.6f%10.6f%10.6f\n',[1 r_prev vnew_1 ]);
%fprintf('%6.0f%11.5f%11.5f%11.5f%10.6f%10.6f%10.6f\n',[2 r_prev vnew_2 ]);
%fprintf('%6.0f%11.5f%11.5f%11.5f%10.6f%10.6f%10.6f\n',[3 r_prev vnew_3 ]);
%fprintf('%6.0f%11.5f%11.5f%11.5f%10.6f%10.6f%10.6f\n',[4 r_prev vnew_4 ]);
%fprintf('%6.0f%11.5f%11.5f%11.5f%10.6f%10.6f%10.6f\n',[5 r_prev vnew_5 ]);

[el_prev,el_next,rv_next]=elements(r1,dv,epoch,nu_new);

```

C. DETERMINATION OF ORBITAL ELEMENTS

```

% First bring in the r and v vectors that you want to convert.
% r is the position vector
% dv is a 5x3 matrix with the velocity vectors for the various delta v's

```

```

function [el_prev,el_next,rv_next] = elements(r,dv,epoch,nu_new)

rl= r;
v1 = dv;

% Constants
rtd=180/pi;
dtr=1/rtd;
I = [1 0 0];
J = [0 1 0];
K = [0 0 1];
AU = 1.4959965e8; % km
TU = 5.0226757e6; % sec
SU = 29.784852; % km/sec
mu = 1; % km^3/sec^2

% Orbit values:
[m n]=size(dv);

for s = 1:m,

% Convert to canonical units
r=rl*1e6/AU;
v=v1(s,:)/SU;
rmag=norm(r);
vmag=norm(v);

% angular momentum
h=cross(r,v);
hmag=norm(h);

% eccentricity vector
e=cross(v,h)-r/rmag;
ecc_n=norm(e);

if ecc_n<1e-10, % Check if eccentricity is zero
e = [0 0 0];
ecc_n=0;
end

% semi-major axis
p = hmag^2/mu;
a = p/(1-ecc_n^2);

% node vector
n = cross(K,h);
nmag=norm(n);
if nmag<1e-10, % Check if inclination is zero
n = [0 0 0];

```

```

nmag=0;
end

% Find the true anomaly at epoch
nu = truanom(r,v,e,n);

% Compute the inclination
inc = incl(h);

% Compute the longitude of ascending node
Omega=lan(n);

% Compute the argument of perigee
omega = aop(n,e,r);

% Compute the rotation matrix
dcm=rot(Omega,inc,omega);

% Compute the eccentric anomaly and mean anomaly
E = acos( (ecc_n + cos(nu*dtr)) / (1+ ecc_n*cos(nu*dtr)) );

if nu>180
    E=2*pi-E;
end

M = (E - ecc_n*sin(E));

H=0;
mu_s=1;
n = sqrt(mu_s/a^3);
global t
M_next = M - n*t;
M_next1 = M_next - fix(M_next/2/pi)*2*pi;
global M_next ecc_n

% Next eccentric anomaly
E_next = fzero('fun1',M_next);

% Compute next true anomaly
nu_next = acos((ecc_n-cos(E_next))/(ecc_n*cos(E_next)-1))*rtd;

if sin(E_next)<0,
    nu_next=360-nu_next;
end
% Compute rmag for next time
rmag_next = a*(1-ecc_n*cos(E_next));

% Compute the r/v at the next time
[r_next v_next]=elip2(rmag_next,nu_new,nu_next,ecc_n,a);
r_next=r_next;
v_next=v_next;

el_prev(s,:)=[a ecc_n Omega inc omega M n E];

```

```

el_next(s,:)=[M_next1 E_next nu_next rmag_next];
rv_next(s,:)=[r_next v_next];
end

```

D. ELIP 1

```

%
% Calculation of the Elliptical/circular orbit
%
%
% LCDR Wade Knudson
% Naval Postgraduate School
% Orbit Visualization Routines
%
% Inputs: rmag,dcm,nu
% User input: a,ecc,newinc
%
% Output: r,v, and nu for the new orbit
%
% Files called: cx,cz
%
% [r,v,nu_new] = elip(rmag,dcm,nu)
%
%
```

```

function [r,v,nu_new,dcm2,ecc] = elip1(rmag,dcm,nu)

% Constants
rtd = 180/pi;
dtr = 1/rtd;
AU = 1.4959965e8; % km
TU = 5.0226757e6; % sec
SU = 29.784852; % km/sec
mu = 1; % km^3/sec^2

%%%%%%%%%%%%%
%
% These are the controlling parameters of the new ellipse
%
%%%%%%%%%%%%%
a=1.1;
ecc=0.1;
r_p=a*(1-ecc);
p= r_p*(1-ecc); %AU /(1-ecc)/AU;

newinc=0;

if ecc == 0, % If circular then no
    % rotation to argument
    % of periapsis (nu_new)
    nu_new = 0;
    a = rmag;
end

```

```

        p = a;
else
    p = a*(1-ecc^2);
    arg=(p/rmag-1)/ecc;

    %if arg-1<1e-10
        %arg=1;
    %end

    nu_new=acos(arg)*rtd;    % true anomaly
end

rp = p/(1+ecc);                      % periapsis
ra = p/(1-ecc);                      % apoapsis

%Perifocal coordinates
r1 = [rmag*cos(nu_new*dtr) rmag*sin(nu_new*dtr) 0];
v1 = sqrt(mu/p)*[-sin(nu_new*dtr) ecc+cos(nu_new*dtr) 0];

h=cross(r1,v1);
e=cross(v1,h)/mu-r/rmag;

% rotate the new orbit to the line of node (-nu), then to desired
inclination,
% and finally rotate nu_2 to get epoch to r.

dcm2= dcm*cz(-nu*dtr)*cx(-newinc*dtr)*cz(nu_new*dtr);
xyz_r=(dcm2*r1)';
r = xyz_r*AU/1e6;
v = (dcm2*v1)''*SU;

```

E. ELIP 2

```

%-----*
%*
%*      Calculation of the Elliptical/circular orbit
%*      *
%*      *
%*      LCDR Wade Knudson
%*      Naval Postgraduate School
%*      Orbit Visualization Routines
%*      *
%*      Inputs:  rmag,dcm,nu
%*      *
%*      Output:  r,v, and nu for the new orbit
%*      *
%*      Files called:  cx,cz
%*      *

```

```

%      [r,v,nu_new] = elip(rmag,dcm,nu)          *
%      *-----*
%
function [r,v] = elip2(rmag,dcm,nu_prev,ecc,a)

% Constants
rtd=180/pi;
dtr=1/rtd;
I = [1 0 0];
J = [0 1 0];
K = [0 0 1];
AU = 1.4959965e8;    % km
TU = 5.0226757e6;    % sec
SU = 29.784852;      % km/sec
mu = 1;              % km^3/sec^2
p = a*(1-ecc^2);
rp = p/(1+ecc);      % periapsis
ra = p/(1-ecc);      % apoapsis

temp = cz(nu_prev*dtr);

r = (temp*[rmag*cos(nu_prev*dtr); rmag*sin(nu_prev*dtr); 0])';
v = (temp*(sqrt(mu/p))*[-sin(nu_prev*dtr); ecc+cos(nu_prev*dtr); 0])';

r=r*AU/1e6;
v=v*SU;

```

F. FUNCTION

```

% Solve Kepler's equation for E
function x = fun(E)
global M_prev ecc_a

x = M_prev - E + ecc_a*sin(E);

```

G. FUNCTION 1

```

% Solve Kepler's equation for E
function [x] = fun1(E)
global M_next ecc_n

x = M_next - E + ecc_n*sin(E);

```

H. PARAM

```

% Solves for a,ecc,Omega,i,omega,nu,E,M,dcm, and rmag from r,v

function [a,ecc,O,inc,o,nu,E,M,dcm,rmag] = param(r1,v1)

% Constants
rtd=180/pi;
dtr=1/rtd;

```

```

I = [1 0 0];
J = [0 1 0];
K = [0 0 1];
AU = 1.4959965e8; % km
TU = 5.0226757e6; % sec
SU = 29.784852; % km/sec
mu = 1; % km^3/sec^2

% Earth values:

r=r1*1e6/AU;
v=v1/SU;
rmag=norm(r);
vmag=norm(v);

% angular momentum
h=cross(r,v);
hmag=norm(h);

% eccentricity vector
e=cross(v,h)-r/rmag;
ecc=norm(e);

if ecc<1e-10, % Check if eccentricity is zero
    e = [0 0 0];
    ecc=0;
end

% node vector
n = cross(K,h);
nmag=norm(n);

if nmag<1e-10, % Check if inclination is zero
    n = [0 0 0];
    nmag=0;
end

% Find the true anomaly at epoch
nu = truanom(r,v,e,n);

% Compute the inclination
inc = incl(h);

%
p = hmag^2/mu;
a = p/(1-ecc^2);

% Compute the longitude of ascending node
O=lan(n);

% Compute the argument of perigee
o = aop(n,e,r);

% Compute the rotation matrix

```

```
dcm=rot(0,inc,o);  
  
E = acos( (ecc + cos(nu*dtr) ) / (1 + ecc*cos(nu*dtr)) );  
M = E - ecc*sin(E);
```

INITIAL DISTRIBUTION LIST

	Number of Copies
1. Defense Technical Information Center 8725 John J. Kingman Rd., STE 0944 Ft. Belvoir, Virginia 22060-6218	2
2. Library, Code 52 Naval Postgraduate School Monterey, California 93943-5101	2
3. Department Chairman, Code AA Department of Aeronautics and Astronautics Naval Postgraduate School Monterey, California 93943-5000	1
4. Department of Aeronautics and Astronautics ATTN: Professor I. M. Ross, Code AA/Ro Naval Postgraduate School Monterey, California 93943-5000	8
5. Space Systems Academic Group ATTN: Professor K. T. Alfriend, Code SP/Al Naval Postgraduate School Monterey, California 93943-5000	2
6. Department of Mathematics ATTN: Professor D. A. Danielson, Code MA/Dd Naval Postgraduate School Monterey, California 93943-5000	1
7. Space Warfare Center/DO ATTN: Deputy Director 720 Irwin Ave. (Stop 82-02) Falcon Air Force Base Colorado Springs, Colorado 80912-7210	1
8. Space Warfare Center/IN ATTN: Deputy Director 720 Irwin Ave. (Stop 82-02) Falcon Air Force Base Colorado Springs, Colorado 80912-7210	1

9. Space Warfare Center/AE 1
ATTN: Deputy Director
720 Irwin Ave. (Stop 82-02)
Falcon Air Force Base
Colorado Springs, Colorado 80912-7210

10. Space Warfare Center/XR 1
ATTN: Deputy Director
720 Irwin Ave. (Stop 82-02)
Falcon Air Force Base
Colorado Springs, Colorado 80912-7210

11. Lieutenant Commander Wade E. Knudson 2
Weapons Test Squadron
Pt. Mugu, California 93042-5001